Field investigations are often hurriedly and carelessly conducted and the incomplete data is then carefully analyzed by precise (out to 08 digit accuracy) computer techniques which produce impressive but erroneous results which in turn lead to inaccurate design assumptions.

— Underwood, (1978)

LANDSLIDE INVESTIGATION 4

Contrary to above quote field investigation has long been recognized as the foremost important and decisive part of a study of landslides and landslide prone regions (Philbrick and Cleaves, 1958; Sowers and Royster, 1978). Landslide investigations mainly revolve around four basic principles that have evolved over many years of experience (Rib and Liang, 1978) viz.

1. Most landslides potential failures can be predicted if proper investigations are performed in time.

2. The cost of preventing landslides is less than the cost of correcting them except for small landslides, which can be handled through normal maintenance.

3. Massive landslides that may cost many times the cost of original facility should be prevented and;

4. The occurrence of initial slope movement can lead to additional unstable conditions and movements.

76

The landslide investigation had been planned based on following elements

- ➢ Formulation of investigation
- ➢ Data collection
- ➢ Data interpretation
- ➢ Application of analysis techniques, and
- ➢ Hazard Zonation and Suggestive Mitigatory Measures.

The entire study has been aimed at carrying out an in-depth investigation of Mangti Landslide environ for recognition of actual or potential slope movements and identification of the type and causes of the movement to put forward appropriate procedures for the prevention or correction of landslides.

The processes involved in slope movements comprise a continuous series of events from cause to effect. The three distinct broad types of landslide processes as outlined by Varnes (1978) are –

a. ***Increase shear stresses*** *– Shear stresses can be increased by processes that lead to removal of lateral support, by the imposition of surcharges, by transitory stresses resulting from explosions or earthquakes and by uplift or tilting of the land surface.*

b. ***Contribute to low strength*** *– Low strength of the earth or rock materials that make up a landslide may reflect inherent material characteristics or may result from the presence of discontinuities within the soil or rock mass.*

c. ***Reduce material strength*** *–Exposure to cyclic changes in extreme temperature causes weathering of clay and disintegration of rocks by formation of desiccation cracking of weak or weathered rock along pre-existing discontinuities, such as bedding planes. Also wet weather may dissolve natural rock cements that hold particles together. Saturation with water reduces effective intergranular pressure and friction and destroys capillary tension.*

The onsite engineering geological investigation had been organized to collect various primary, secondary and collateral data on physical and anthropogenic (biological) environmental domains to evaluate the above mentioned processes. The information gathered can be grouped into two categories – Conditioning Factors and Triggering Factors. Details on various studied parameters under these factors includes:-

Conditioning Factors

The rock and regolith, their composition, thickness, size, structural fabric, relative position; position of partings with respect to topography (relief, slope, height and landform attributes), long term processes like weathering that influences the slope stability.

Triggering Factors

These factors generally determine the temporal occurrence of landslides. The information on the most responsible natural landslide triggers gathered in the study area are about earthquake shaking, intense rainfall, water-level change and pore water pressure, human activities such as excavation for road cuts, overloading, blasting, overgrazing and deforestation.

By assessing causes of and factors contributing to slope movement, surface observation and geologic mapping of slopes provide the basis for subsurface investigations and engineering analyses that follow. Accurate interpretation of the surface features of a landslide can be used to evaluate the mode of movement, judge the direction and rate of movement, and estimate the geometry of the slip surface.

On-site engineering-geologic investigations of Mangti Landslide Environ includes engineering-geologic mapping, rock and slope mass characterization (RMR and SMR), field instrumentation and kinematic study of Mangti Landslide Region and RMR and SMR of entire Tawaghat – Jipti (T-J) Route Corridor.

ENGINEERING GEOLOGIC MAPPING OF MANGTI LANDSLIDE

The Mangti Landslide falls within the domain of Higher Himalayas and located (30°00'15"N; 80°43'07"E) about 2km north of MCT and in the proximity of Mangti Village (Figure 1.1). The Mangti landslide constitutes a part of one of the most severely affected landslide zones in Uttarakhand State. A highway stretch of about 48 km between Dharchula – Tawaghat – Mangti (Jipti) is known for its intense landslide activities. This Mangti landslide represents a typical case of *multi-rotational slip* and currently passing through its 3rd Phase. Its geological characteristics, tectonic position as well as slow repetitive mobility, makes it the most ideal case for in-depth study. A sketch of ground surface profile of landslide highlighting its characteristics is given in Figure 4.1.

The engineering-geologic mapping of the Mangti Landslide is carried out with a view to document surface conditions to provide a basis for projecting subsurface conditions that in-turn would assist in the slope stability analysis. The entire exercise has been focused on to delineate landslide geometry features, geomorphic attributes, regolithic material, bedrock exposures and surface-water features.

Figure 4.1 - Ground Surface Profile and Phases of Activation of Mangti Landslide
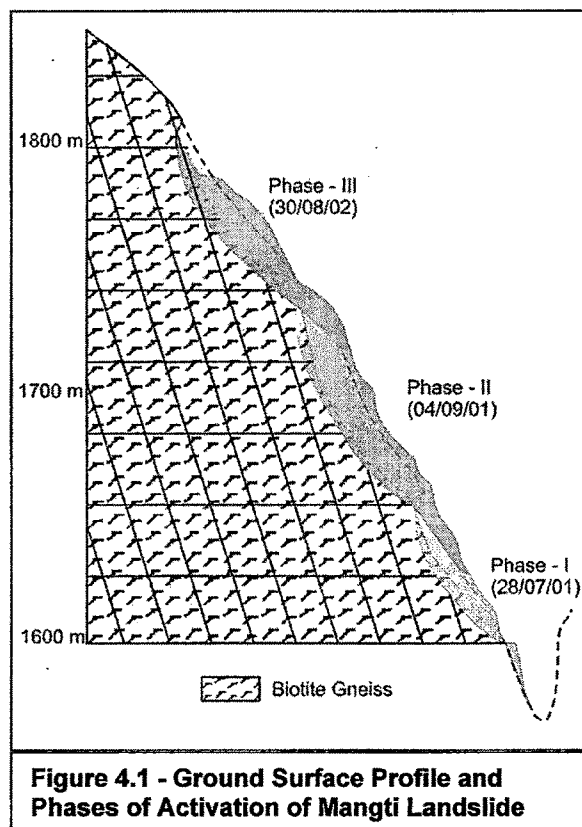
GEOLOGICAL ENVIRONMENT

The Mangti Landslide has developed within the regolithic mass of biotite gneiss rocks belonging to Higher Himalayan Crystallines. The rocks exposed in landslide vicinity are predominantly biotite gneisses with a thin band of amphibolite and biotite schist. Major outcrops are concealed in the toe portion of the landslide region (Figure 4.2).

Under hand specimen the biotite gneiss shows the presence of quartz and feldspar, with platy muscovite and biotite minerals. At places quartz and feldspar grains are seen forming porphyroblasts around which biotite and muscovite are arranged in a preferred orientation giving rise to eye shaped augen structure. The effect of weathering is very much pronounced and has substantially contributed towards the development of a huge volume of debris mass. The main body of Mangti Landslide is characterized by patchy occurrences of the bedrock, i.e., biotite gneiss. A detailed scan line survey (Priest and Hudson, 1981) of the landslide environ has revealed in all 05 sets of joint system viz.

J_1 (also called as foliation plane joint) – this joint set has dip varying from $25°$ - $64°$ and the amount of dip varies from as low as $12°$ to as high as $70°$.

J_2 – this joint set has dip varying from $110°$ - $150°$ and the dip amount varies from as low as $56°$ to as high as $88°$.

J_3 – this joint set has dip varying from $191°$ - $230°$ and the dip amount varies from as low as $50°$ to as high as $80°$.

J_4 – this joint set has dip varying from $240°$ - $289°$ and the dip amount varies from as low as $54°$ to as high as $80°$.

J_5 – this joint set has dip varying from $308°$ - $350°$ and the dip amount varies from as low as $30°$ to as high as $85°$.

Apart from these major sets of joints there exists other sets of criss-crossing joints, which show their dips in north, south and easterly directions. Presence of these stray joints may be attributed to excessive blasting for the road development, particularly the radiating joints. Based on field data a geological cross section along NE – SW has been constructed incorporating litho-structural inputs and slope attributes (Figure 4.3). Cross section clearly depicts that the beds are dipping away from topographic slope. Therefore, the slope failure (Mangti Landslide) is attributed to development of slip surface through the combination of joint controlled discontinuity surfaces. The topographic profile giving details on various joint planes suggest that the joints having dips $225°$ / $64°$ **(J_3)** and $358°$ / $25°$ **(J_5)** are the causative factors for release of mass at Mangti Landslide.
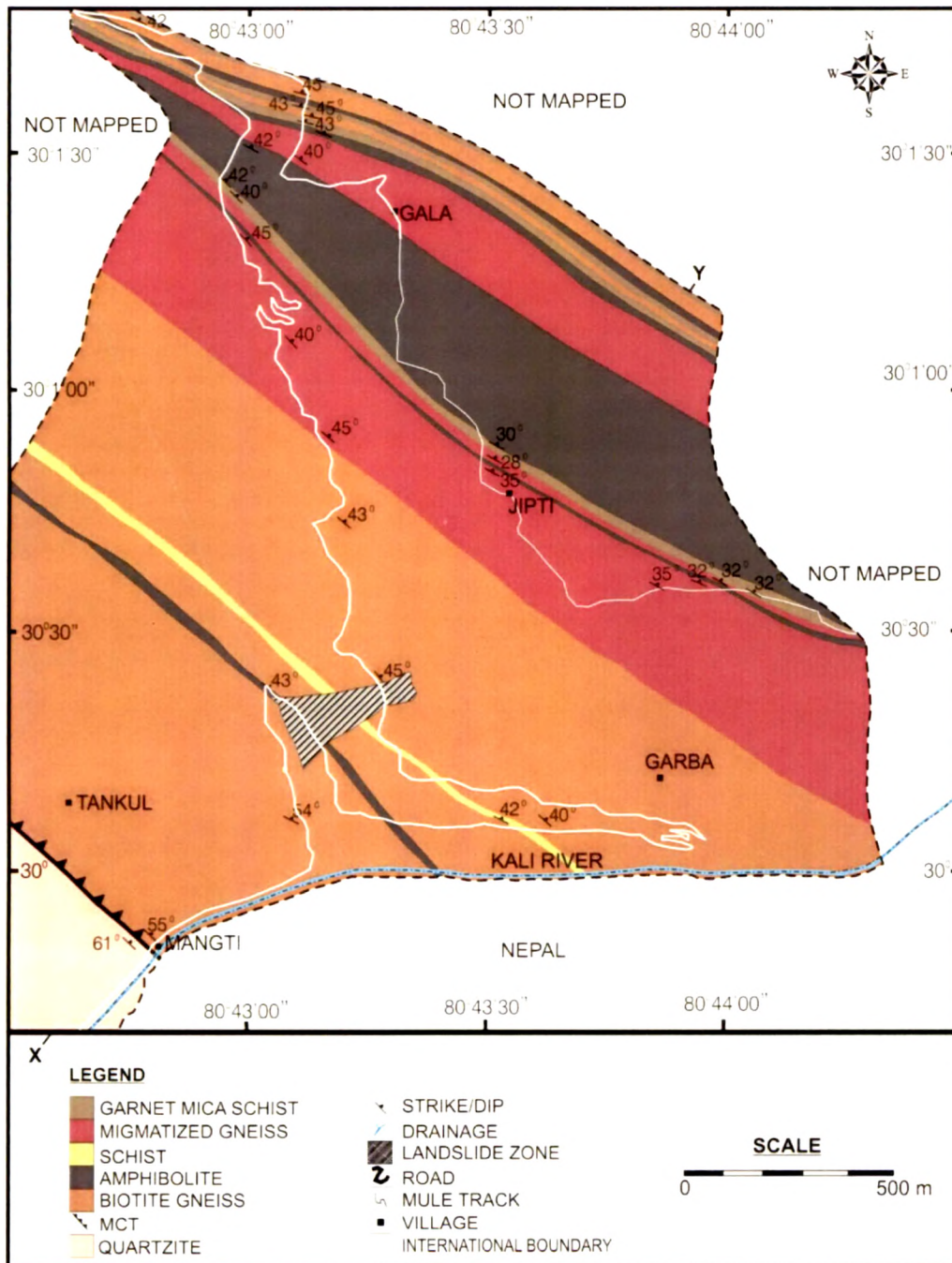
Figure 4.2 - Geological Map of the Mangti Landslide Environ

LEGEND

- GARNET MICA SCHIST
- MIGMATIZED GNEISS
- SCHIST
- AMPHIBOLITE
- BIOTITE GNEISS
- MCT
- QUARTZITE

SCALE

0 100 200 300 400 500 m

200 m

JIPTI

SHYAMKHOLA GAD

LANDSLIDE ZONE

MANGTI

MCT

2600 m

1400 m

1600m
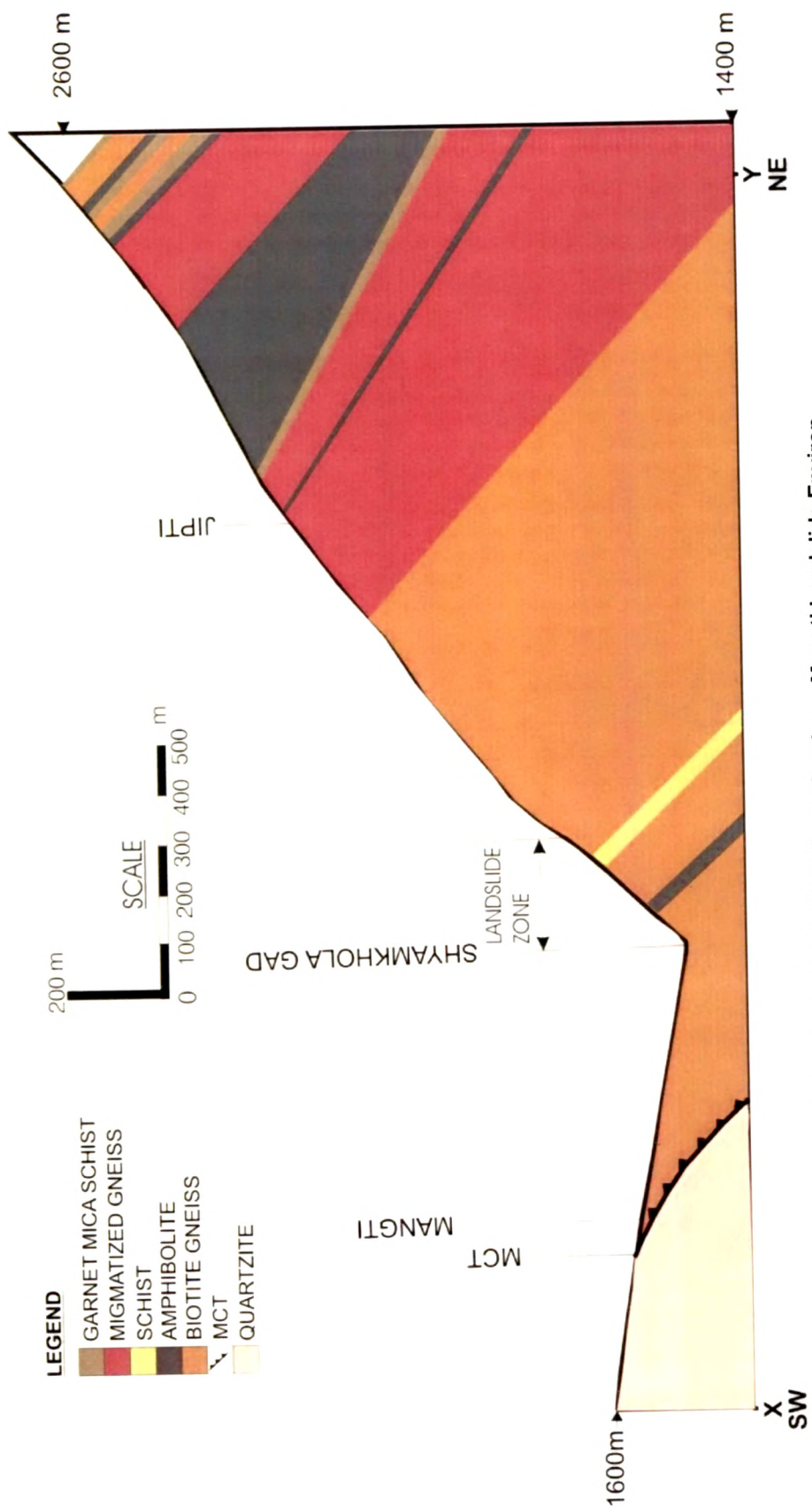
X
SW

Y
NE

Figure 4.3 - Geological Cross Section – Mangti Landslide Environ

82

GROUND SURVEY AND ALTIMETRIC CHARACTERISTION

Study of topography at a landslide site often provides the first indications of potential instability and the degree to which the area has undergone landslide activity. Since a landslide activity is very much site specific, its characterization at large scale requires development of contour plan at 01m interval, encompassing the area of landslide in proper and its adjacent stable shoulder regions. In order to prepare 01m contour plan a permanent local bench mark at the proximity of landslide in BRO − GREF Camp site was established. Further a sub-system of additional bench mark platforms networked in triangulation were established on either sides of shoulder ridges, at toe, mid-body and above crown regions of the landslide (Plate IV.1A) so that they can be used as ready references for subsequent monitoring activities (Figure 4.4). The levels were measured and transferred to the additional bench mark platforms using Leica make Electronic Total Station (TC-307) with an angular accuracy of ±4 seconds (Plate IV.1B&C). This was followed by establishment of a closed spaced 5x5m reference grids demarcated using wooden pegs (Plate IV.1D). By sighting the optical prism from this grid based wooden pegs as well as positions of various features viz. road alignment, trees, rock outcrops, cracks, subsidence zone, field level points of landslide surface from the established local bench marks the complete ground survey of the Mangti Landslide was carried out. The data thus acquired with the help of Total Station were then transferred onto a computer and were processed using AutoCAD-2004 software. The final 01m contour plan was developed from the point data downloaded using TRIMBLE GEOMATIC OFFICE Software.

Thus, based on developed contour plan and recorded landslide attributes all geometrical parameters of the landslide were determined and have been tabulated in Table − 4.1. Also a topographical cross-section of Mangti Landslide depicting landslide surface and discontinuity planes has been prepared (Figure 4.5).

Depth of landslide could not be estimated owing to absence of sub-surface information. However, there exists empirical methods, which can provide broad idea about this, viz.

a. The depth of movement at the centre of the slide is rarely greater than the width of the zone of surface movement, and

b. The maximum depth of the failure surface is often approximately equal to the distance from the break in original ground surface slope to the most uphill crack or scarp (McGuffey, 1991).

Table 4.1 - Geometric Parameters of Mangti Landslide

Altimetric Details (m)			Landslide Zone			Slip Area Dimension (m)	
Crown	Toe	Tip	Total Area	Length	Breadth	Breadth	Length
1800	1600	1570	11.66 Hectare. (Including adjacent shoulder region)	580m	Toe 200 m	Toe 125	400
					Body 235 m	Body 135	
					Top 125 m	Crown 35	

The Mangti Landslide may be placed into Deep Slide (5 – 20m) category of Zaruba and Mencl (1969) that has been judged considering slope of the landslide scarp and intact rock exposed on the shoulders, therefore, the landslide depth of **20**m has been adopted for other relevant studies.
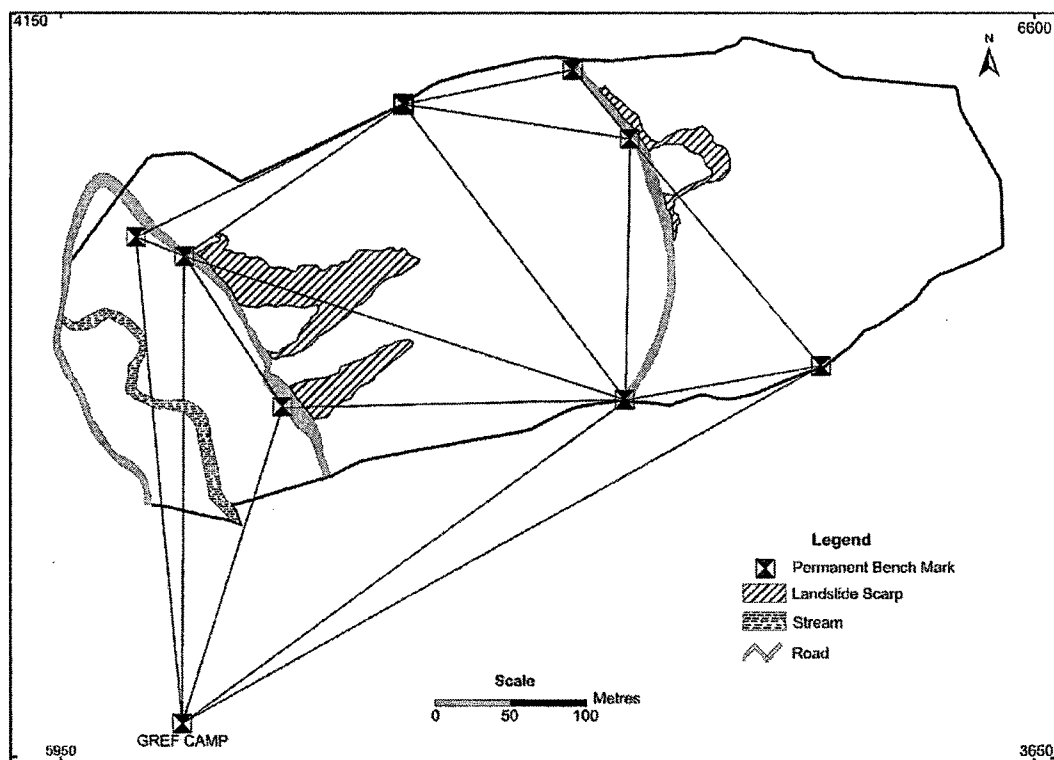
Figure 4.4 – Map Showing Triangulation Network of Bench Marks Established at Mangti Landslide

A. Construction of 3'x3' concrete permanent Bench Mark on stable ground

B. Total Station being setup for transferring of levels to the permanent bench marks

C. Optical Prism being sighted to the Total Station for mapping road and recording other landslide attributes

D. Development of 5x5m reference grid of wooden pegs in the active landslide zone

Plate IV.1 - Field Photographs of Different Stages in Ground Survey Carried out at Mangti Landslide

85
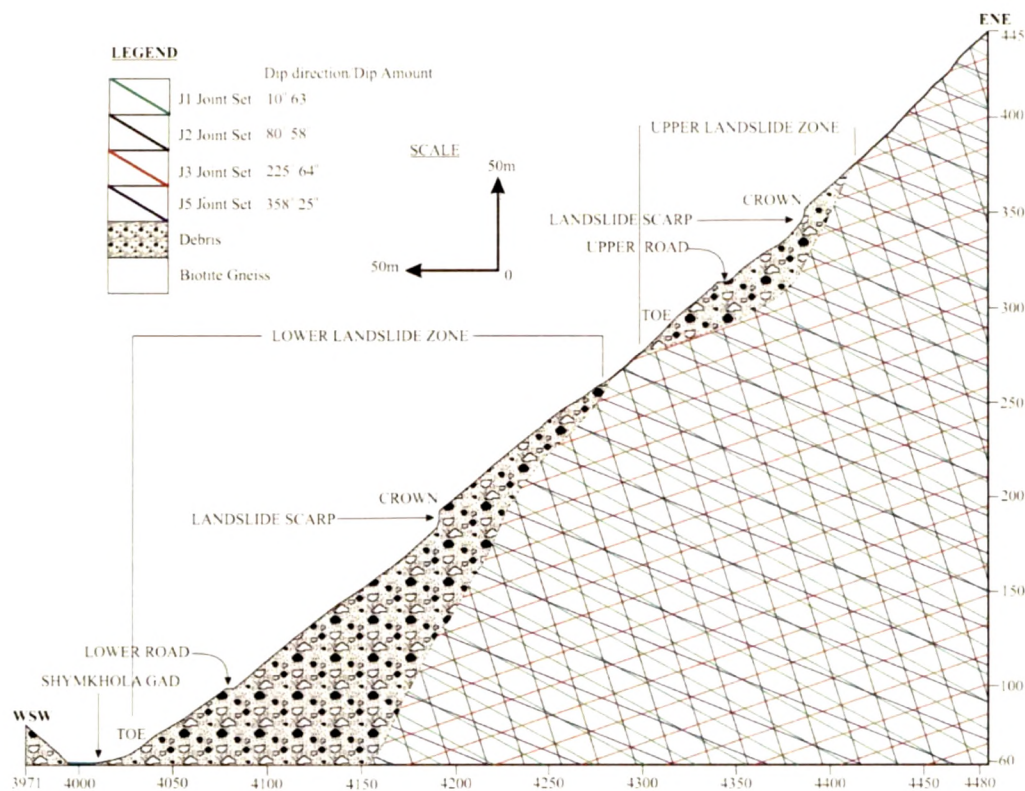
Figure 4.5 - Morpho-Structural Cross Section of Mangti Landslide

SURFACE OBSERVATIONS OF MANGTI LANDSLIDE

Features on the ground surface are the key to understand landslide processes and causative factors. In landslide evaluation systematic study and inventory of the various landslide features, their geometry and nature of the sliding surface are among the most important to understand the sub-surface conditions. Based on field observations and measurements of various surface features through Total Station, a comprehensive landslide map has been prepared (Figure 4.6). Mangti landslide zone has been studied from the point of view of its material characteristics that are observed along crown, scarp, body, sides' scarp, toe-sides' scarp, zone of ablation and zone of accumulation (Plate IV.2). Measured dimensional parameters of these scarp geometries are given in Table – 4.2. Representative disturbed and un-disturbed samples were collected by driving core cutters/UDS tubes as per Indian Standard prescribed procedures. The details on their Granulometric and engineering characteristics are discussed under Laboratory Studies.

86

Table 4.2 - Element Characteristics of the Mangti Landslide

Scarp Geometry	Sides	Depth (m)	Angle	Material Characteristics
Crown Scarp	Left	2.00	Vertical	Sharp, un-vegetated colluvial material with predominance of medium sand, presence of sub-surface drainage-potholes, etc.
	Right	3.00	Vertical	Soil followed by colluvial material showing imbrications.
Zone of Ablation	Left	15.91	38°–45°	Colluvial material with patches of bouldery debris. Ground surface is sharp, un-vegetated.
	Right	18.28	48°	
Body Sides' Scarp	Left	3 – 3.75	Vertical	Sharp, thin soil horizon followed by bouldery colluvial material, tilted trees on shoulder surface.
	Right	1.53 – 2.13	35° – 40°	Sharp, thick soil horizon followed by pebbly horizon with silty-clayey ad-mixture.
Toe Sides' scarp	Left	3 – 4.52	---	Thick gravelly, pebbly material with sandy matrix.
	Right	1.25 – 2.72	---	Thick coarse sandy material with intercalation of gravels.
Zone of Accumulation	Un-drained and drained depressions; hummocky topography, angular blocks, un-vegetated with isolated presence of in-situ bedrock blocks.			

ROCK AND SLOPE MASS CHARACTERIZATION

For proper understanding of slope failure and its mechanism, in-depth study of rock and soil mass is pre-requisite. Further, behaviour of slope mass and its vulnerability to fail depends upon material characteristics encompassing parameters like composition, deformational characteristics, presence of discontinuities and their nature, susceptibility of weathering and land use pattern. Amongst all, material composition and discontinuity surfaces play vital role in enhancing vulnerability of slope failure.

A detailed quantitative and qualitative investigation of the Mangti Landslide environ has been carried out employing an established technique of 'Scanline Survey' (Priest & Hudson, 1981).
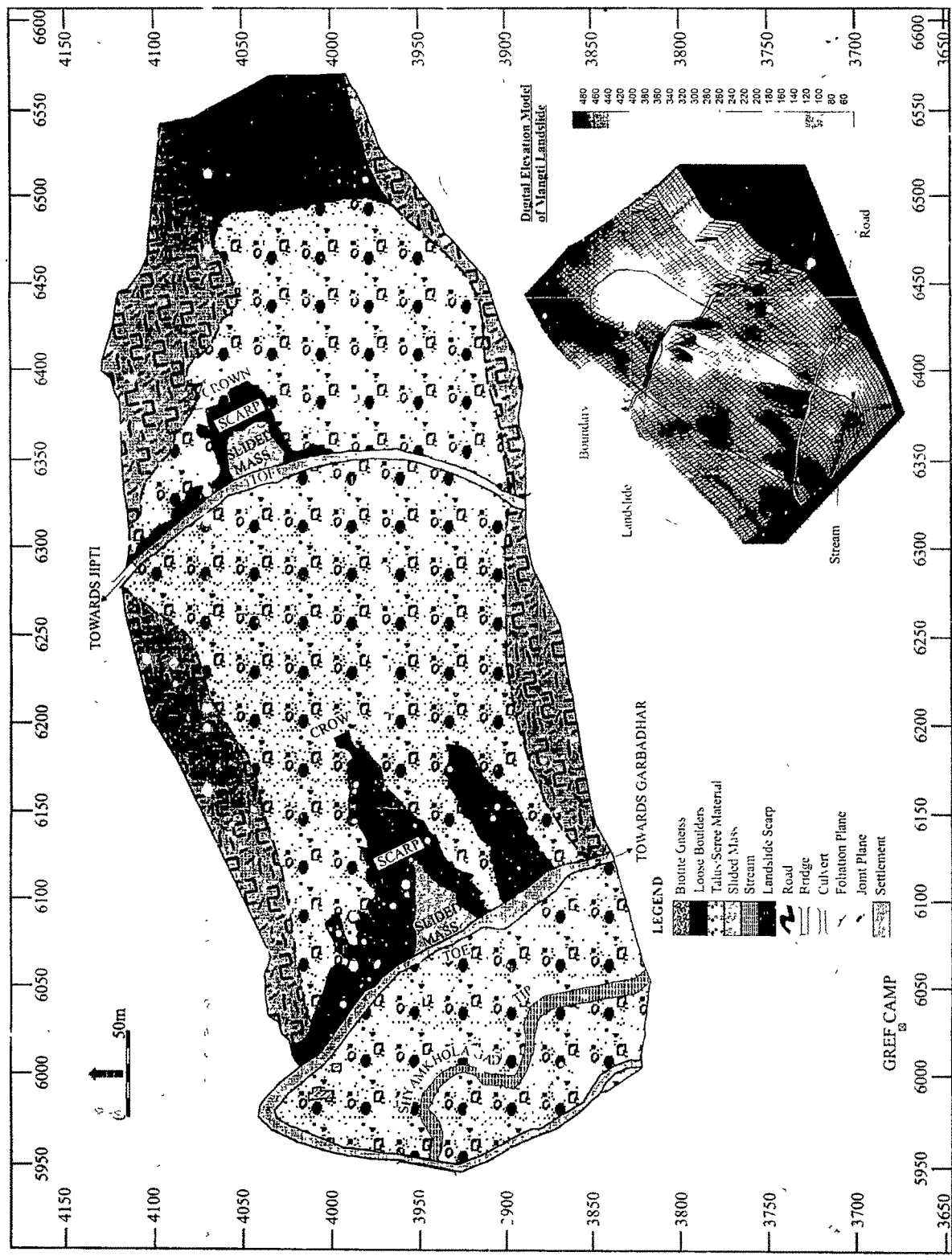
Figure 4.6 – Geomorphic Attributes and DEM of Mangti Landslide

B. View of crown scarp and accumulation zone

D. Close view of crown scarp sediments showing massive sized boulders embedded with coarse sand matrix

Plate IV.2 – contd....

A. View of landslide ablation zone

C. Tilting of trees seen on left shoulder of Mangti Landslide indicating slow creep movement

E. View of left side flank scarp showing imbrications in slump mass
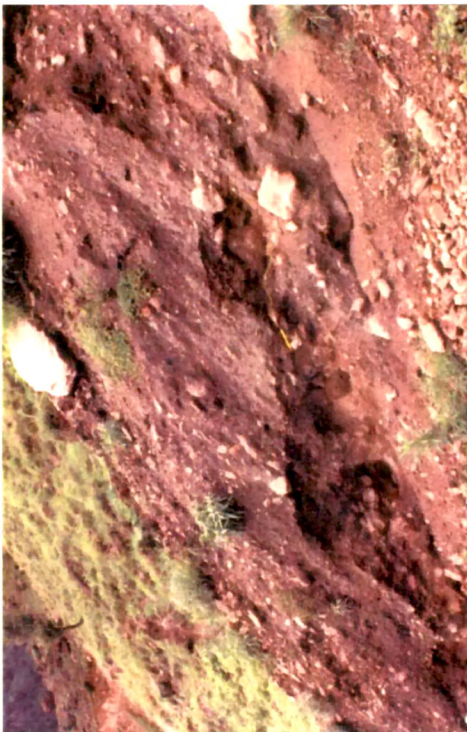
E. Close view of right flank scarp sediments

E. View of downside landslide comprising of boulder and gravel size rocks intermixed with coarse sand matrix

Plate IV.2 - Field Photographs of Different Surface Features Mapped on Mangti Landslide

For the mapping purpose, especially to make inventory of litho-specific discontinuity surfaces, the following rationales were adopted –

❖ Scan line survey of every **30**m length at the interval of **500**m and/or change in lithology, whichever is earlier for Tawaghat – Jipti Route Corridor. Whereas, for Mangti Landslide including shoulder region entire stretch of **800**m has been mapped.

❖ Inventory of lithology and measurement of various joint sets, foliation plane, etc.

❖ Inventory of joint conditions based on Bieniawski (1989) Classification.

❖ Plotting of lithological contacts and discontinuity parameters at **1:100** scale

❖ Collection of rock samples and discontinuity infilling material for detailed engineering geological characterization through laboratory studies.

❖ Measurement of in-field Unconfined Compressive Strength (UCS) using Schmidt's Concrete Hammer.

Slope Mass Rating (SMR) proposed by Romana, 1993 has been proved to be a very useful tool for the preliminary assessment of slope stability. It provides some simple guidelines about instability modes and the required support measures. SMR classification is a subsequent development of the Bieniawski 'Rock Mass Rating' (RMR) system which has become known worldwide, and applied by many technicians as a systematic tool to describe rock mass conditions. The RMR concept has been proved to be useful in assessing the need for support system, particularly in tunnel studies. Where as the SMR system provides adjustment factors, field guidelines and recommendations on support methods which allow a systematic use of geomechanical classification for slopes.

RMR CHARACTERIZATION OF MANGTI LANDSLIDE REGION

The **RMR Geomechanic Classification** of rock incorporates *five* parameters viz.

1. Strength of Intact Rock Material

Adequate input data for the strength of intact rock is the Uniaxial Compressive Strength. Bieniawski uses the classification of the UCS of intact rock proposed by Deere and Miller (1966) and reproduced in Table 4.3. Intact rock strength was tested in the

field with the help of a 'Schmidt Impact Hammer'. While carrying out this test care was taken on choosing the outcrop with proper smooth surface, flat and free from cracks and discontinuities to a depth of 6cm. Anomalous test results were discarded whenever there was lack of rebound, hollow sound or if it caused minor cracks or visible failure. Uniformly 20 tests/per rock unit were carried out for the different rock units avilable along TJRC. Further, consecutive test locations were kept separate by at least one diameter of the hammer. The angle of orientation of the hammer was noted every time and appropriate correction curves were referred from the calibration charts supplied with the instrument. The re-bound index was thus obtained by taking the median value of the 20 test results.

2. *Rock Quality Designation (RQD)*

RQD is defined by Deere (1964) as the total length of all the pieces of sound core over 10 cm long, expressed as a percentage of the length drilled. As it was not possible to have drill cores, RQD was estimated using emperical method (Palmstrom,1975), which is based on joint count (Equation- 1).

Equation 1 gives an approximate correlation between RQD and the volumetric joint count (number of joints per cubic meter)

$$RQD = 115 - 3.3Jv \ (RQD > 100) \qquad\qquad (1)$$

$$Jv = \sum 1 / \overline{S_i}$$

Where $\overline{S_i}$ is the mean spacing for the discontinuities of family i (m).

3. *Spacing of Joints*

Spacing of discontinuities is the distance between them, measured along a line perpendicular to discontinuity planes. The ISRM (1978) suggest the use of minimum, modal and maximum values of spacing to characterize a set of joints. This procedure has been superseded in practice by the use of mean spacing. Bieniawski (1989) defines the spacing as the 'mean distance' so the mean spading is the appropriate input in RMR and SMR classification. Spacing is measured with a tape along the rock outcrop, counting the number of joints in a fixed distance and multiplying by the corresponding cosines of angles between the normal to joints and the plane of rock outcrop. RMR uses the classification of discontinuity spacings proposed by the ISRM (1978) Table 4.3.

4. Condition of Joints

This parameter accounts for the separation or aperture of joints, their continuity, the surface roughness, the wall condition (hard or soft), and the presence or absence of in-filling materials in the joints. Various category groups describing the joint condition is shown in Table 4.3.

5. Ground Water Condition

Groundwater conditions can be estimated in RMR geomechanical classification in three different ways: (i) inflow of water in tunnels; (ii) pore pressure ratio; and (iii) general conditions. For slopes the general conditions are usually sufficiently adequate. The ISRM (1978) has proposed a seepage classification and same has been adapted to classify surfacing joints to assess groundwater conditions (Table 4.3).

Based on detailed inventory of observed discontinuity surfaces and their characterization using RMR Classification criteria various Scanline maps were prepared (**ANNEXURE – 1**). A sample case of prepared Scanline map is given in Figure 4.7. Field data inputs on Scanline survey have been recorded on specifically prepared pro forma (**ANNEXURE – 2**). The RMR values derived for the Mangti landslide region are given in Table 4.4.

Although the Mangti Landslide and its adjoining shoulder regions are predominantly characterized by biotite gneissic rock with stray occurrences of thin schistose bands; the RMR computed for 800m long stretch show considerable variation ranging from 00 – 75. However, overall condition of the rock masses fall within III to IV Classes signifying fair to poor condition. Scanline stretch exhibiting poor rock quality at times is attributed to excessive blasting carried out by BRO for road development. Scanline segments giving zero RMR (Class – V) are predominantly occupied by thick regolithic and talus/scree materials; there by indicates most vulnerable regions for slope failure.
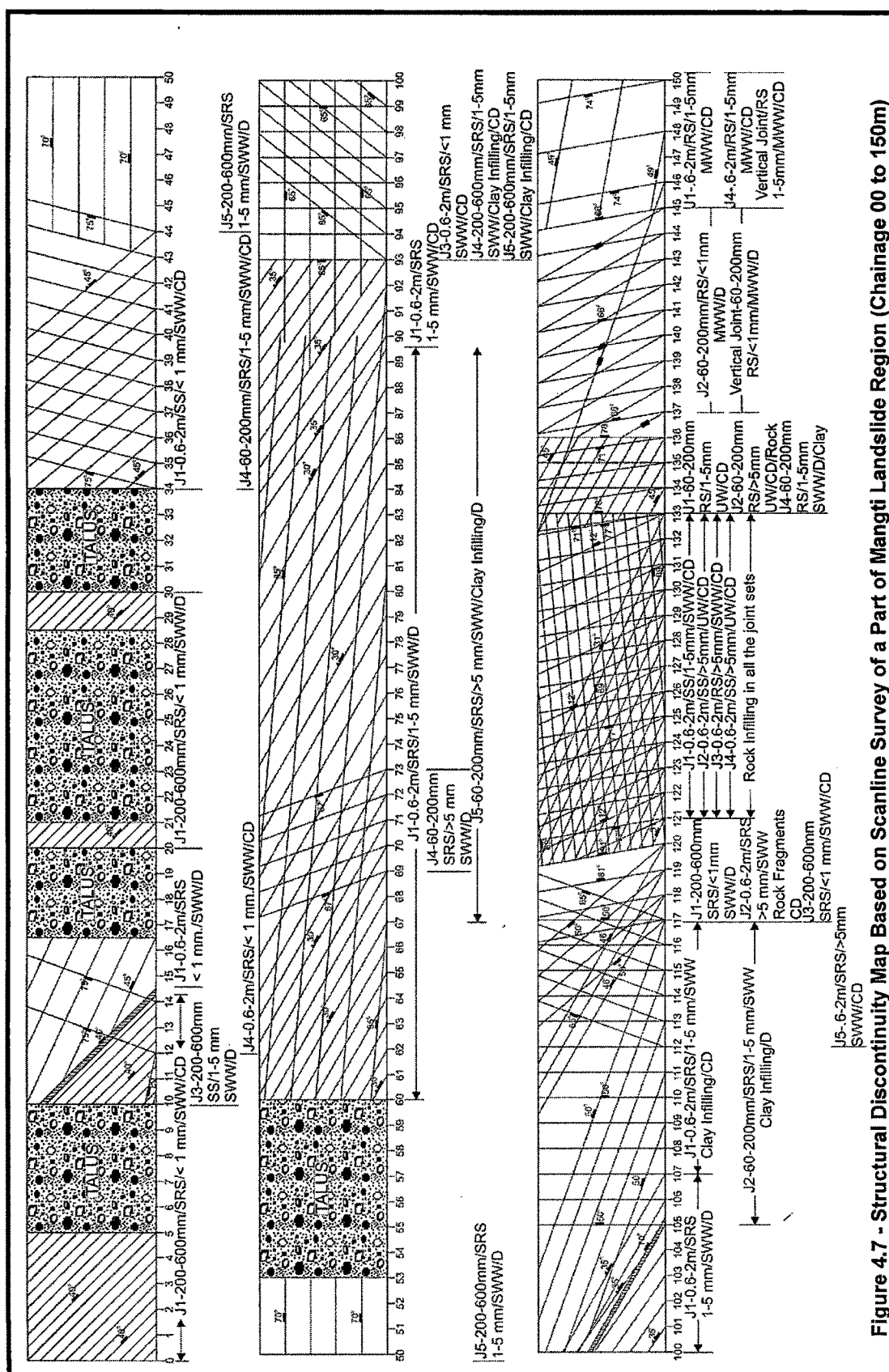
Figure 4.7 - Structural Discontinuity Map Based on Scanline Survey of a Part of Mangti Landslide Region (Chainage 00 to 150m)

Table 4.3 - Rock Mass Rating System (After Bieniawski 1989)

A. CLASSIFICATION PARAMETERS AND THEIR RATINGS

Parameter		Range of values						
1	Strength of intact rock material	Point-load strength index	>10 MPa	4 - 10 MPa	2 - 4 MPa	1 - 2 MPa	For this low range - uniaxial compressive test is preferred		
		Uniaxial comp. strength	>250 MPa	100 - 250 MPa	50 - 100 MPa	25 - 50 MPa	5 - 25 MPa	1 - 5 MPa	< 1 MPa
	Rating		15	12	7	4	2	1	0
2	Drill core Quality RQD		90% - 100%	75% - 90%	50% - 75%	25% - 50%	< 25%		
	Rating		20	17	13	8	3		
3	Spacing of discontinuities		> 2 m	0.6 - 2 . m	200 - 600 mm	60 - 200 mm	< 60 mm		
	Rating		20	15	10	8	5		
4	Condition of discontinuities (See E)		Very rough surfaces Not continuous No separation Unweathered wall rock	Slightly rough surfaces Separation < 1 mm Slightly weathered walls	Slightly rough surfaces Separation < 1 mm Highly weathered walls	Slickensided surfaces or Gouge < 5 mm thick or Separation 1-5 mm Continuous	Soft gouge >5 mm thick or Separation > 5 mm Continuous		
	Rating		30	25	20	10	0		
5	Ground water	Inflow per 10 m tunnel length (l/m)	None	< 10	10 - 25	25 - 125	> 125		
		(Joint water press)/ (Major principal σ)	0	< 0.1	0.1, - 0.2	0.2 -0.5	> 0.5		
		General conditions	Completely dry	Damp	Wet	Dripping	Flowing		
	Rating		15	10	7	4	0		

B. RATING ADJUSTMENT FOR DISCONTINUITY ORIENTATIONS (See F)

Strike and dip orientations		Very favourable	Favourable	Fair	Unfavourable	Very Unfavourable
Ratings	Tunnels & mines	0	-2	-5	-10	-12
	Foundations	0	-2	-7	-15	-25
	Slopes	0	-5	-25	-50	

C. ROCK MASS CLASSES DETERMINED FROM TOTAL RATINGS

Rating	100 ← 81	80 ← 61	60 ← 41	40 ← 21	< 21
Class number	I	II	III	IV	V
Description	Very good rock	Good rock	Fair rock	Poor rock	Very poor rock

D. MEANING OF ROCK CLASSES

Class number	I	II	III	IV	V
Average stand-up time	20 yrs for 15 m span	1 year for 10 m span	1 week for 5 m span	10 hrs for 2.5 m span	30 min for 1 m span
Cohesion of rock mass (kPa)	> 400	300 - 400	200 - 300	100 - 200	< 100
Friction angle of rock mass (deg)	> 45	35 - 45	25 - 35	15 - 25	< 15

E. GUIDELINES FOR CLASSIFICATION OF DISCONTINUITY conditions

Discontinuity length (persistence)	< 1 m	1 - 3 m	3 - 10 m	10 - 20 m	> 20 m
Rating	6	4	2	1	0
Separation (aperture)	None	< 0.1 mm	0.1 - 1.0 mm	1 - 5 mm	> 5 mm
Rating	6	5	4	1	0
Roughness	Very rough	Rough	Slightly rough	Smooth	Slickensided
Rating	6	5	3	1	0
Infilling (gouge)	None	Hard filling < 5 mm	Hard filling > 5 mm	Soft filling < 5 mm	Soft filling > 5 mm
Rating	6	4	2	2	0
Weathering	Unweathered	Slightly weathered	Moderately weathered	Highly weathered	Decomposed
Ratings	6	5	3	1	0

F. EFFECT OF DISCONTINUITY STRIKE AND DIP ORIENTATION IN TUNNELLING**

Strike perpendicular to tunnel axis		Strike parallel to tunnel axis	
Drive with dip - Dip 45 - 90°	Drive with dip - Dip 20 - 45°	Dip 45 - 90°	Dip 20 - 45°
Very favourable	Favourable	Very unfavourable	Fair
Drive against dip - Dip 45-90°	Drive against dip - Dip 20-45°	Dip 0-20 - Irrespective of strike°	
Fair	Unfavourable	Fair	

* Some conditions are mutually exclusive . For example, if infilling is present, the roughness of the surface will be overshadowed by the influence of the gouge. In such cases use A.4 directly.
** Modified after Wickham et al (1972).

Table 4.4 - Rock Mass Rating (RMR) Classification of Mangti Landslide Region
(Based on Beineawski, 1989)

Stretch	UCS Rating	RQD Rating	Spacing of Discont. Rating	Condit. of Discont. Rating	Ground Water Condi. Rating	R M R	Class	Remarks
0-5	4	17	10	25	15	71	II	Good
5-10	0	0	0	0	0	0	V	Very Poor
10-17	4	20	10	10	10	54	III	Fair
17-20	0	0	0	0	0	0	V	Very Poor
20-21	4	20	5	25	10	64	II	Good
21-28.5	0	0	0	0	0	0	V	Very Poor
28.5-30	4	20	5	25	10	64	II	Good
30-34	0	0	0	0	0	0	V	Very Poor
34-40	7	20	8	10	15	65	II	Good
40-44	7	20	8	10	15	65	II	Good
44-53	7	20	10	10	10	57	III	Fair
53-60	0	0	0	0	0	0	V	Very Poor
60-67	7	20	15	10	10	62	II	Good
67-69	7	17	8	0	10	42	III	Fair
69-73	7	13	8	0	10	38	IV	Poor
73-90	7	17	8	10	10	52	III	Fair
90-93	7	20	15	10	15	67	II	Good
93-105	7	3	10	25	15	60	III	Fair
105-117	7	8	8	0	10	33	IV	Poor
117-120	7	13	10	10	15	55	III	Fair
120-133	7	13	15	0	15	50	III	Fair
133-136	7	13	10	0	10	40	IV	Poor
136-145	7	13	10	20	10	60	III	Fair
145-155	7	13	15	10	15	60	III	Fair
155-159	7	20	15	0	15	57	III	Fair
159-180	7	13	8	20	15	63	II	Good
180-197	0	0	0	0	0	0	V	Very Poor
197-216	7	13	8	0	10	38	IV	Poor
216-220	7	17	15	25	15	75	II	Good
220-270	0	0	0	0	0	0	V	Very Poor
270-290	7	13	8	10	15	53	III	Fair
290-326	7	8	8	10	15	48	III	Fair
326-394	0	0	0	0	0	0	V	Very Poor
394-432	Mangti Landslide encountered in this Stretch along the Road Side							
437-580	0	0	0	0	0	0	V	Very Poor
580-595	4	8	8	0	15	35	IV	Poor
595-635	0	0	0	0	0	0	V	Very Poor
635-765	This stretch is highly disturbed because of Blasting induced fractures and joints							
765-811	4	13	8	0	15	40	IV	Poor

SMR CHARACTERIZATION OF MANGTI LANDSLIDE REGION

As it has already been elucidated that RMR alone cannot provide any concrete clues about the behaviour of rock masses resting over slopes, therefore, computed RMR need to be adjusted by giving appropriate weightage of various slope attributes. To come over with these limitations Romana (1993) had developed a supplementary classification, i.e., Slope Mass Rating (SMR).

The **'Slope Mass Rating' (SMR)** is obtained from RMR by subtracting a factorial adjustment factor depending on the joint – slope relationship and adding a factor depending on the method of excavation. The SMR is calculated using the following Equation 2 –

$$SMR = RMR + (F1 . F2 . F3) + F4 \qquad\qquad (2)$$

The RMR is computed according to Bieniawski's (1989) approach that has a total range of 0 - 100. The adjustment rating for joints (Table 4.5) is the product of three factors as follows:

(i) F_1 depends on parallelism between joints and slope face strikes. Its range is from 1.00 (when both are near parallel) to 0.15 (when the angle between them is more than $30°$ and the failure probability is very $10°$). These values were established empirically, but afterwards were found to approximately match the relationship

$$F_1 = (1 - \sin A)^2$$

Where, A denotes the angle between the strikes of the slope face and the joint.

(ii) F_2 refers to joint dip angle in the planar mode of failure. In a sense it is a measure of the probability of joint shear strength. Its value varies from 1.00 (for joints dipping more than $45°$) to 0.15 (for joints dipping less than $20°$). Also established empirically, it was found afterwards to match approximately the relationship

$$F^2 = tg^2 \beta_j$$

Where, β_j denotes the joint dip angle. For the toppling mode of failure $F2$ remains 1.00.

(iii) F_3 reflects the relationship between the slope face and joint dip. Bieniawski's 1976 figures have been kept. In the planar mode of failure F_3 refers to the probability that joints 'daylight' in the slope face. Conditions are fair when slope face and joints are parallel. When the slope dips 10° more than joints, very unfavourable conditions occur. For the toppling mode of failure, unfavourable or very unfavourable conditions cannot happen in view of the nature of toppling, as there are very few sudden failures and many toppled slopes remain standing.

The adjustment factor for the method of excavation (Table 4.6) has been fixed empirically as follows:

(i)   Natural slopes are more stable, because of long time erosion and built-in protection mechanisms (vegetation, crust desiccation, etc.): $F_4 = +15$.

(ii) Presplitting increases slope stability for half a class: $F_4 = \pm 10$.

(iii) Smooth blasting, when well done, also increases slope stability: $F_4 = \pm 8$.

(iv) Normal blasting, applied with sound methods, does not change slope stability: $F_4 = 0$.

(v) Deficient blasting, often with too much explosive, no detonation timing and/or non-parallel holes, damages stability: $F_4 = -8$.

(vi) Mechanical excavation of slopes, usually by ripping, can be done only in soft and/or fractured rock, and is often combined with some preliminary blasting. The method neither increases nor decreases slope stability: $F_4 = 0$.

A tentative description of SMR classes is given in Table 4.7.

Obtained SMR for Mangti Landslide and its adjacent shoulder regions (Table 4.8) by and large fall within SMR Class IV and V, characterized by *Unstable – Completely Unstable* Stability Categories. Such deteriorated state of SMR is attributed to –

i.   Biotite Gneisses, which is dominated by argillaceous minerals prone to enhanced weathering;

ii. High frequency of jointing; and their trends;

iii. Excessive and uncontrolled blasting and ;

iv. Predominance of Talus / Scree materials over the slopes.

Further, although the rock dip is opposite to slope direction, its angular relationship with slope and the joints that are day lighting towards valley slopes have produced unfavourable conditions for a typical planar and wedge failure.

Table 4.5 - Adjustment Rating for Joints

Case		Very favorable	Favorable	Fair	Unfavorable	Very unfavorable
P	$|\alpha_j - \alpha_s|$	>30°	30-20°	20-10°	10-5°	5°
T	$|(\alpha_j - \alpha_s) - 180°|$					
P/T	F_1	0.15	0.40	0.70	0.85	1.00
P	$|\beta_j|$	<20°	20-30°	30-35°	35-45°	45°
P	F_2	0.15	0.40	0.70	0.85	1.00
T	F_2	1	1	1	1	1
P	$\beta_j - \beta_s$	>10°	10-0°	0°	0° to 10°	<-10°
T	$\beta_j - \beta_s$	<110°	110-120°	>120°	-	-
P/T	F_3	0	-6	-25	-50	-60

P, plane failure; T, toppling failure; α_j, joint dip direction; α_s slope dip direction; β_j, joint dip; β_s slope dip

Table 4.6 - Adjustment Rating for Methods of Excavation of Slopes

Method	Natural Slope	Presplitting	Smooth blasting	Blasting or mechanical	Deficient blasting
F_4	+15	+10	+8	0	-8

Table 4.7 - Tentative Description of SMR Classes

Class	SMR	Description	Stability	Failures	Support
I	81-100	Very good	Completely stable	None	None
II	61-80	Good	Stable	Some blocks	Occasional
III	41-60	Normal	Partially stable	Some joints or many wedges	Systematic
IV	21-40	Bad	Unstable	Planar or big wedges	Important/corrective
V	0-20	Very bad	Completely unstable	Big planar or soil-like	Reexcavation

Table 4.8 - Slope Mass Rating (SMR) Classification of Mangti Landslide Region Based on Romana, 1993.

Stretch	RMR	F1	F2	F3	F4	SMR	SMR Class	Slope Mass Description Based On Derived Rating
RIGHT SHOULDER REGION								
0-5m	71	S1 - 0.15	S1 - 0.85	S1 - 60	- 8	55	III	Normal
5-10m	0	0	0	0	0	0	V	Very Bad
10-17m	54	S1 - 0.15 S2 - 0.15 S3 - 0.15 S4 - 0.15	S1 - 0.85 S2 - 1 S3 - 1 S4 - 1	S1 - -60 S2 - -50 S3 - 0 S4 - 0	- 8	38	IV	Bad
17-20m	0	0	0	0	0	0	V	Very Bad
20-21m	64	S1 - 0.15 S2 - 0.15	S1 - 1 S2 - 1	S1 - -60 S2 - -50	- 8	47	III	Normal
21-28.5m	0	0	0	0	0	0	V	Very Bad
28.5-30m	64	S1 - 0.15	S1 - 0.85	S1 - -60	- 8	48	III	Normal
30-34m	0	0	0	0	0	0	V	Very Bad
34-40m	65	S1 - 0.15 S2 - 0.15	S1 - 1 S2 - 1	S1 - -50 S2 - 0	- 8	49	III	Normal
40-44m	65	S1 - 0.15	S1 - 1	S1 - -50	- 8	49	III	Normal
44-53m	57	S1 - 0.15 S2 - 0.15	S1 - 1 S2 - 1	S1 - -50 S2 - 0	- 8	41	III	Normal
53-60m	0	0	0	0	0	0	V	Very Bad
60-67m	62	S1 - 0.15	S1 - 0.70	S1 - -60	- 8	47	III	Normal
67-69m	42	S1 - 0.15	S1 - 1	S1 - -6	- 8	33	IV	Bad
69-73m	38	S1 - 0.15	S1 - 1	S1 - 0	- 8	30	IV	Bad
73-90m	52	S1 - 0.15	S1 - 1	S1 - 0	- 8	44	III	Normal
90-93m	67	S1 - 0.15	S1 - 0.70	S1 - -60	- 8	52	III	Normal
93-105m	60	S1 - 0.15 S2 - 0.15 S3 - 0.15	S1 - 1 S2 - 1 S3 - 1	S1 - 0 S2 - 0 S3 - 0	- 8	52	III	Normal
105-117m	33	S1 - 0.15 S2 - 0.15 S3 - 0.15 S4 - 0.15	S1 - 1 S2 - 1 S3 - 1 S4 - 1	S1 - -50 S2 - 0 S3 - -50 S4 - 0	- 8	17	V	Very Bad
117-120m	55	S1 - 0.40 S2 - 0.15 S3 - 0.15	S1 - 1 S2 - 1 S3 - 1	S1 - -50 S2 - -50 S3 - 0	- 8	27	IV	Bad
120-133m	50	S1 - 0.15 S2 - 0.15 S3 - 0.40 S4 - 0.15	S1 - 0.70 S2 - 0.15 S3 - 1 S4 - 1	S1 - -60 S2 - -60 S3 - 0 S4 - -60	- 8	33	IV	Bad
133-136m	40	S1 - 0.15 S2 - 0.15 S3 - 0.15	S1 - 1 S2 - 1 S3 - 1	S1 - -50 S2 - 0 S3 - 0	- 8	24	IV	Bad
136-145m	60	S1 - 0.15 S2 - 0.15	S1 - 1 S2 - 1	S1 - 0 S2 - 0	- 8	52	III	Normal
145-155m	60	S1 - 0.15 S2 - 0.15 S3 - 0.15 S4 - 0.15	S1 - 1 S2 - 1 S3 - 1 S4 - 1	S1 - 0 S2 - 0 S3 - -50 S4 - 0	- 8	44	III	Normal

155-159m	57	S1 – 0.15	S1 – 1	S1 – 0	- 8	49	III	Normal
159-180m	63	S1 – 0.15 S2 – 0.15 S3 – 0.15 S4 – 0.15	S1 – 1 S2 – 1 S3 – 1 S4 – 1	S1 – -50 S2 – 0 S3 – -6 S4 - -6	- 8	47	III	Normal
180-197m	0	0	0	0	0	0	V	Very Bad
197-216m	38	S1 – 0.15 S2 – 0.15 S3 – 0.70	S1 – 0.40 S2 – 1 S3 – 1	S1 – -60 S2 – 0 S3 – 0	- 8	26	IV	Bad
216-220m	75	S1 – 0.85 S2 – 0.40 S3 – 0.40	S1 – 1 S2 – 1 S3 – 1	S1 – -6 S2 – 0 S3 – 0	- 8	61	II	Good
220-270m	0	0	0	0	0	0	V	Very Bad
270-290m	53	S1 – 0.15 S2 – 0.15	S1 – 1 S2 – 1	S1 – -50 S2 – 0	- 8	37	IV	Bad
290-326m	48	S1 – 0.15 S2 – 0.70 S3 – 0.15	S1 – 0.85 S2 – 1 S3 – 1	S1 – -50 S2 – 0 S3 – 0	- 8	33	IV	Bad
326-394m	0	0	0	0	0	0	V	Very Bad
394-432m	**Mangti Landslide encountered in this Stretch along the Road Side**							
LEFT SHOULDER REGION								
437-580m	0	0	0	0	0	0	V	Very Bad
580-595m	35	S1 – 0.15 S2 – 0.15 S3 – 0.85	S1 – 1 S2 – 0.40 S3 – 1	S1 – 0 S2 – -60 S3 – 0	- 8	23	IV	Bad
595-635m	0	0	0	0	0	0	V	Very Bad
635-765m	**This stretch is highly disturbed because of Blasting induced fractures and joints**							
765-811m	40	S1 – 0.15 S2 – 0.85 S3 – 0.15	S1 – 0.40 S2 – 1 S3 – 1	S1 – -60 S2 – 0 S3 – 0	- 8	28	IV	Bad

GEO-MECHANICAL STUDY OF T – J ROUTE CORRIDOR

Tawaghat – Jipti Route Corridor (TJRC) is riddled with numerous landslides that are reactivated every year during monsoon season and causes considerable damage to the corridor higway. Road construction along this stretch was initiated in year 1993 and now it has reached to last phase of construction. With a view to characterize natural slope material and also the influence of road building activity on reactivation of unstable areas, Scanline Survey (Priest & Hudson, 1981) was carried out for the entire route corridor. A scanline segment of 30m was investigated approximately every 500m throughout the road length. Also for every variation in lithology the inventory of rock/slope mass was carried out to derive SMR for the T-J Route Corridor. Figure 4.8 and Plate IV.3A-D, shows the location of scanline survey observation sites in the TJRC and detailed Scanline Maps are presented in

101

ANNEXURE – 3. The Geo-mechanical studies of this corridor using Scanline approach and subsequent rock discontinuity characterization has provided very scintillating results on RMR-SMR categorization. RMR-SMR classification of various Scanline segments (Table 4.9 & 4.10) clearly depicts that majority of discontinuity induced rock and slope masses fall within III – IV and V rating classes.

Further, SMR of rocks (Table 4.10) belonging to Chiplakot and Higher Himalayan Crystalline mass predominantly fall within IV and V class ratings and all such segments are chronically affected by landslide hazards. Whereas, SMR of rocks belonging to Sirdang Sedimentary Zone by and large falls within Normal (Class-III) and Bad (Class-IV) ratings. Here, majority of schistose rocks fall in Bad Category and competent quartzitic and calcareous rocks in Normal Category. The assigned SMR values signifying Very Bad (Class V) and Bad (Class IV) conditions of slope masses could be attributed to deterioration of rock mass under the process of shallow, progressive physical and chemical alteration and its subsequent detachment and removal or re-distribution by transport agents (Nicholson, 2004). Further, deterioration occurs because of excavation particularly, blasting disturbs the rock mass by releasing confinement, leading to expansive recovery under ambient environmental conditions (Gerber & Scheidegger, 1969; Nichols, 1980).

FIELD INSTRUMENTATION

Landslides often present the ultimate measurement challenges, in part because of their initial lack of definition and the sheer scale of the problems. Intuitively, there is a desire to quantify the extent of a potential or real disaster, but what should be measured? The answer can be complicated and should be addressed by drawing on the best available information concerning topography, geology, groundwater and material properties. The measurement problem usually requires information ranging from a coarse scale down to a fine scale and involving a number of instrumentation techniques. While dealing with landslide hazards the ultimate goal is to select the most sensitive measurement parameters, the ones that will change significantly at the onset of the landslide event.
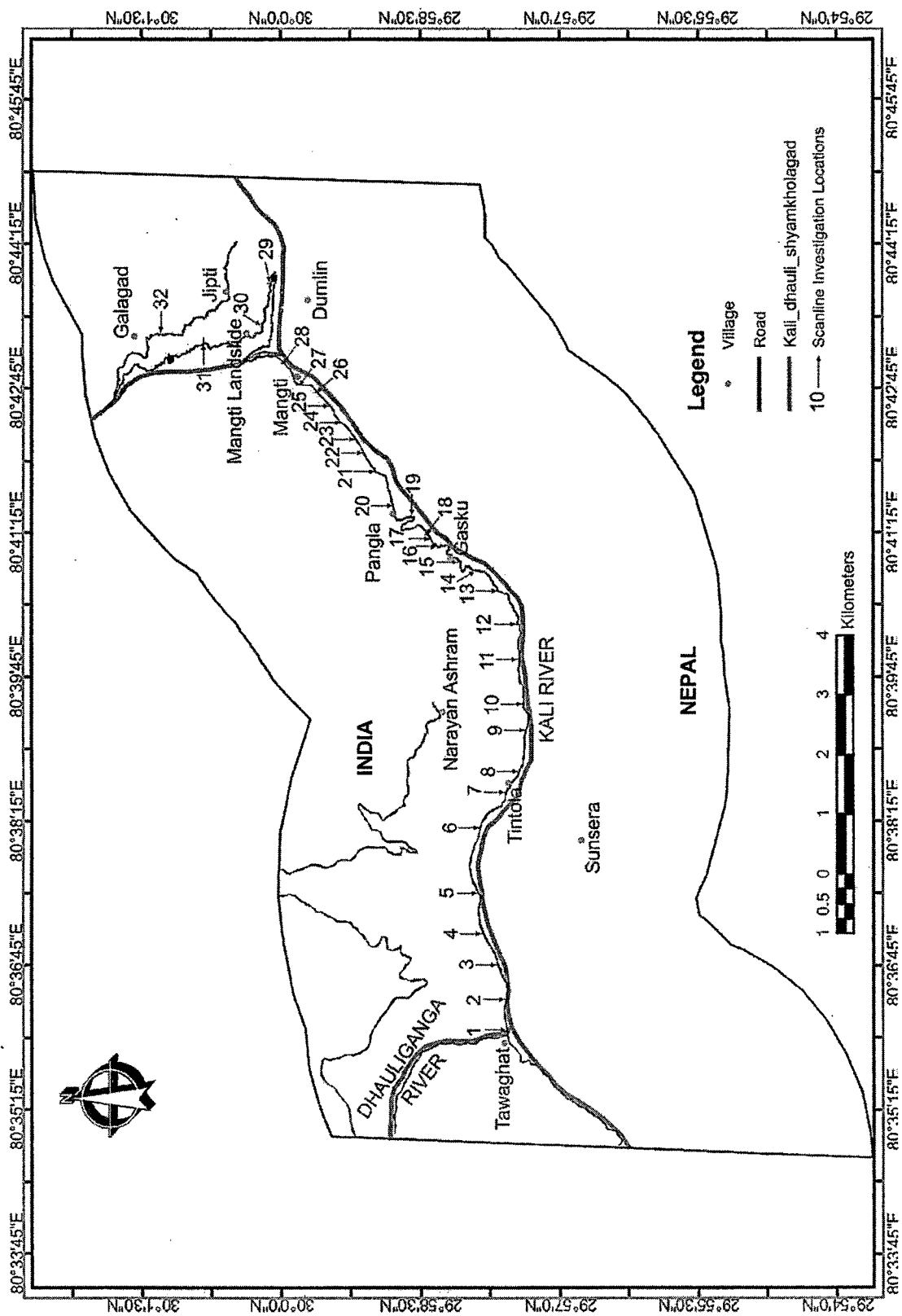
Figure 4.8 - Location Map of Scanline Survey Observation Sites along TJRC

103

A. Field photograph of Scanline Survey carried out at stretch no. 32 (geo. Lat/lon- 30°01'17.696" N & 80°43'19.093" E)

B. Field photograph of Scanline Survey carried out at stretch no. 29 (geo. Lat/lon- 30°00'06.232" N & 80°43'50.984" E)

C. Field photograph of Scanline Survey carried out at stretch no. 25 (geo. Lat/lon- 29°59'28.782" N & 80°42'33.681" E)

D. Field photograph of Scanline Survey carried out at stretch no. 08 (geo. Lat/lon- 29°57'26.002" N & 80°38'45.878" E)

Plate IV.3 - Field Photographs of Some Selective Sites of Scanline Survey Investigation along TJRC

104

Table 4.9 - Rock Mass Rating (RMR) Classification of Tawaghat – Jipti Route Corridor (Based on Bieniawski, 1989)

Stretch	UCS Rating	RQD Rating	Spacing of Discont. Rating	Cond. of Discont. Rating	Ground Water Condi. Rating	RMR	RMR Class	Rock Mass Description Based on Derived Rating
CHIPLAKOT CRYSTALLINE MASS								
Stretch-1 Tawaghat	4	20	10	25	15	74	II	Good Rock
Stretch-2	4	8	10	10	15	47	III	Fair Rock
Stretch-3	4	20	15	10	10	59	III	Fair Rock
Stretch-4	4	20	15	30	15	84	I	Very Good Rock
Stretch-5	4	20	10	10	10	54	III	Fair Rock
Stretch-6	4	20	8	25	15	72	II	Good Rock
Stretch-7	4	17	8	0	10	39	IV	Poor Rock
Stretch-8	4	17	15	30	15	81	I	Very Good Rock
Stretch-9	4	13	15	25	15	72	II	Good Rock
Stretch-10	4	17	8	10	15	54	III	Fair Rock
Stretch-11	4	13	8	25	15	65	II	Good Rock
Stretch-12	4	20	8	25	10	67	II	Good Rock
Stretch-13	4	20	15	25	4	68	II	Good Rock
Stretch-14	4	20	15	10	7	56	III	Fair Rock
Stretch-15	4	17	10	0	10	41	III	Fair Rock
SIRDANG SEDIMENTARY ZONE								
Chlorite Schist	2	8	5	10	15	40	IV	Poor Rock
Quartzite	7	3	5	30	15	60	III	Fair Rock
Chlorite Schist	2	3	5	10	15	35	IV	Poor Rock
Amphibolite	7	20	8	20	15	70	II	Good Rock
Chlorite Schist	2	13	5	10	4	34	IV	Poor Rock
Amphibolite	4	20	8	20	15	67	II	Good Rock
Chlorite Schist	2	13	5	10	4	34	IV	Poor Rock
Quartzite	7	3	5	20	15	50	III	Fair Rock
Chlorite schist	2	8	5	10	15	40	IV	Poor Rock
Carbo-phyllite	7	13	8	25	15	68	II	Good Rock
Quartzite	7	17	8	25	15	72	II	Good Rock
Calcsilicate Rock	4	17	8	20	15	64	II	Good Rock
Talc-Chlorite Schist	0	3	5	0	15	23	IV	Poor Rock
Phyllite	4	13	5	10	15	47	III	Fair Rock
Graphite Schist	4	13	5	10	15	47	III	Fair Rock
Garnetiferous Schist	4	8	5	10	15	42	III	Fair Rock
Calc-Schist	4	13	15	20	15	67	II	Good Rock
Quartzite	7	13	8	25	15	68	II	Good Rock
Carbo phyllite	4	13	8	25	15	65	II	Good Rock
Flaggy quartzite	0	3	5	10	15	33	IV	Poor Rock
Calcschist	4	8	8	20	15	55	III	Fair Rock
Flaggy	4	8	8	20	4	44	III	Fair Rock

105

Quartzite

Calcschist	4	8	8	20	10	50	III	Fair Rock
Chlorite schist	2	8	5	10	10	35	IV	Poor Rock
Quartzite	7	17	8	25	4	61	II	Good Rock
Amphibolite	7	17	8	25	15	72	II	Good Rock
Quartzite	7	17	8	25	15	72	II	Good Rock
Chlorite Schist	2	8	5	10	15	40	IV	Poor Rock
Amphibolite	7	20	15	25	15	82	I	Very Good Rock
Chlorite Schist	4	8	5	10	15	40	IV	Poor Rock
Quartzite	7	20	8	25	10	67	II	Good Rock
Amphibolite	4	20	8	25	10	67	II	Good Rock
Quartzite	7	20	8	25	4	64	II	Good Rock
Amphibolite	4	13	8	25	15	65	II	Good Rock
Quartzite	7	13	8	25	15	68	II	Good Rock

HIGHER HIMALAYAN CRYSTALLINES

Biotite Gneiss	4	20	10	10	10	54	III	Fair Rock
Amphibolite	4	13	8	10	15	50	III	Fair Rock
Migmatised Gneiss	7	20	20	25	15	87	I	Very Good Rock
Amphibolite	4	20	15	20	4	63	II	Good Rock
GM Schist	2	3	5	10	4	24	IV	Poor Rock
Amphibolite	4	20	15	20	4	63	II	Good Rock
Biotite Gneiss	4	13	8	10	10	45	III	Fair Rock
Amphibolite	4	20	15	20	4	63	II	Good Rock
Migmatised Gneiss	7	20	20	25	15	87	I	Very Good Rock
Biotite Gneiss	4	13	8	10	10	45	III	Fair Rock
GM Schist	2	3	5	10	4	24	IV	Poor Rock
Amphibolite	4	20	15	20	4	63	II	Good Rock
Biotite Gneiss	4	13	8	10	10	45	III	Fair Rock
GM Schist	2	3	5	10	4	24	IV	Poor Rock

Table 4.10 - Slope Mass Rating (SMR) Classification of Tawaghat - Jipti Route Corridor (Based on Romana, 1993)

Stretch	RMR	F1	F2	F3	F4	SMR	SMR Class	Slope Mass Description Based On Derived Rating
CHIPLAKOT CRYSTALLINES								
Stretch-1 Tawaghat	74	S1 – 0.15 S2 – 0.15 S3 – 0.15 S4 – 0.15 S5 – 0.15 S6 – 0.15	S1 – 0.40 S2 – 1 S3 – 1 S4 – 1 S5 – 1 S6 – 1	S1 – -60 S2 – -50 S3 – -60 S4 – -60 S5 – -50 S6 – -60	- 8	57	III	Normal
Stretch-2	47	S1 – 0.15 S2 – 0.15 S3 – 0.15 S4 – 0.40 S5 – 0.15	S1 – 0.85 S2 – 1 S3 – 1 S4 – 1 S5 – 0.70	S1 – -60 S2 – -60 S3 – -60 S4 – -60 S5 – -60	- 8	15	V	Very Bad
Stretch-3	59	S1 – 0.15	S1 – 0.15	S1 – -60	-8			

		S2 – 0.15	S2 – 0.40	S2 - -60		47	III	Normal
		S3 – 0.15	S3 – 1	S3 – 0				
Stretch-4	84	S1 – 0.15	S1 – 1	S1 - -60	-8			
		S2 – 0.15	S2 – 1	S2 - -25				
		S3 – 0.15	S3 – 1	S3 - -50		67	II	Good
		S4 – 0.15	S4 – 1	S4 - -60				
Stretch-5	54	S1 – 0.15	S1 – 0.70	S1 - -60	-8			
		S2 – 0.15	S2 – 1	S2 - -50				
		S3 – 0.15	S3 – 1	S3 - -60		37	IV	Bad
Stretch-6	72	S1 – 0.15	S1 – 1	S1 - -60	-8			
		S2 – 0.15	S2 – 1	S2 - -50		4	V	Very Bad
		S3 – 1	S3 – 1	S3 - -60				
		S4 – 0.15	S4 – 1	S4 – 0				
Stretch-7	39	S1 – 0.15	S1 – 0.85	S1 - -50	-8			
		S2 – 0.15	S2 – 1	S2 - -50				
		S3 – 1	S3 – 1	S3 - -6		23	IV	Bad
		S4 – 0.15	S4 – 1	S4 – 0				
Stretch-8	81	S1 – 0.15	S1 – 1	S1 - -6	-8			
		S2 – 0.15	S2 – 1	S2 – 0				
		S3 – 1	S3 – 1	S3 - -6		65	II	Good
		S4 – 0.15	S4 – 0.7	S4 - -6				
		S5 – 0.15	S5 – 1	S5 - -50				
Stretch-9	72	S1 – 0.15	S1 – 1	S1 - -50	-8			
		S2 – 0.15	S2 – 1	S2 – 0				
		S3 – 1	S3 – 1	S3 - -25		39	IV	Bad
		S4 – 0.15	S4 – 1	S4 – 0				
Stretch-10	54	S1 – 0.15	S1 – 1	S1 - -50	-8			
		S2 – 0.15	S2 – 1	S2 – 0				
		S3 – 0.15	S3 – 0.85	S3 - -60		38	IV	Bad
Stretch-11	65	S1 – 0.15	S1 – 1	S1 - -50	-8			
		S2 – 0.15	S2 – 1	S2 - -6				
		S3 – 0.15	S3 – 0.85	S3 - -60		14	V	Very Bad
		S4 – 0.15	S4 – 1	S4 - -6				
		S5 – 0.70	S5 – 1	S5 - -50				
		S6 – 0.85	S6 – 1	S6 - -50				
Stretch-12	67	S1 – 0.15	S1 – 1	S1 - -50	-8			
		S2 – 0.15	S2 – 1	S2 – 0				
		S3 – 0.15	S3 – 0.70	S3 - -60		51	III	Normal
Stretch-13	68	S1 – 0.15	S1 – 0.85	S1 - -60	-8			
		S2 – 0.40	S2 – 1	S2 - -50		40	IV	Bad
		S3 – 0.15	S3 – 0.70	S3 - -60				
		S4 – 0.15	S4 – 1	S4 – 0				
		S5 – 0.15	S5 – 1	S5 – 0				
Stretch-14	56	S1 – 0.15	S1 – 1	S1 - -6	-8			
		S2 – 0.15	S2 – 1	S2 – 0				
		S3 – 0.15	S3 – 0.85	S3 - -50		41	III	Normal
		S4 – 0.15	S4 – 1	S4 - -6				
Stretch-15	41	S1 – 0.15	S1 – 1	S1 - -60	-8			
		S2 – 0.15	S2 – 1	S2 - -50				
		S3 – 0.15	S3 – 1	S3 - -60		24	IV	Bad

SIRDANG SEDIMENTARY ZONE

Chlorite Schist	40	S1 – 0.15	S1 – 1	S1 - -6	-8			
		S2 – 0.15	S2 – 1	S2 – 0				
		S3 – 0.15	S3 – 1	S3 - -6		31	IV	Bad
Quartzite	60	S1 – 0.15	S1 – 0.85	S1 - -60	-8			

Table 4.10 – contd....

		S2 – 0.15	S2 – 1	S2 – 0				
		S3 – 0.15	S3 – 1	S3 - -50				
		S4 – 0.85	S4 – 1	S4 - -6				
		S5 – 0.15	S5 – 1	S5 – 0		44	III	Normal
		Shear-pl-0.15	Shear-pl-0.85	Shear-pl--60				
Chlorite Schist	35	S1 – 0.15	S1 – 1	S1 - -60	0			
		S2 – 0.70	S2 – 1	S2 - -50		0	V	Very Bad
		S3 – 0.15	S3 – 1	S3 - -60				
Amphibolite	70	S1 – 0.15	S1 – 0.85	S1 - -60	-8			
		S2 – 0.15	S2 – 1	S2 – 0		53	III	Normal
		S3 – 0.15	S3 – 1	S3 - -60				
Chlorite Schist	34	S1 – 0.15	S1 – 0.85	S1 - -50	0	27	IV	Bad
		S2 – 0.7	S2 – 1	S2 – 0				
		S3 – 0.15	S3 – 1	S3 - -6				
Amphibolite	67	S1 – 0.15	S1 – 0.85	S1 - -60	-8	51	III	Normal
		S2 – 0.15	S2 – 1	S2 – 0				
		S3 – 0.15	S3 – 1	S3 - -50				
Chlorite Schist	34	S1 – 0.15	S1 – 0.85	S1 - -60	0	25	IV	Bad
		S2 – 0.40	S2 – 1	S2 – 0				
		S3 – 0.15	S3 – 1	S3 - -60				
Quartzite	50	S1 – 0.15	S1 – 1	S1 - -60	-8			
		S2 – 0.15	S2 – 1	S2 - -6				
		S3 – 0.15	S3 – 1	S3 - -60		33	IV	Bad
Chlorite schist	40	S1 – 0.15	S1 – 1	S1 – 0	0			
		S2 – 0.15	S2 – 1	S2 – 0				
		S3 – 0.15	S3 – 0.85	S3 – 0		40	IV	Bad
Carbo-phyllite	68	S1 – 0.15	S1 – 1	S1 - -6				
		S2 – 0.15	S2 – 1	S2 – 0				
		S3 – 0.15	S3 – 0.85	S3 - -6	-8	59	III	Normal
Quartzite	72	S1 – 0.15	S1 – 1	S1 - -6				
		S2 – 0.15	S2 – 1	S2 – 0				
		S3 – 0.15	S3 – 0.4	S3 - -60	-8	60	III	Normal
Calc-silicate Rock	64	S1 – 0.15	S1 – 1	S1 - -25				
		S2 – 0.70	S2 – 1	S2 – 0				
		S3 – 0.40	S3 – 0.85	S3 - -60	-8	35	IV	Bad
Talc-Chlorite Schist	23	S1 – 0.15	S1 – 1	S1 – 0	+1			
		S2 – 0.70	S2 – 1	S2 – 0				
		S3 – 0.15	S3 – 0.85	S3 - -6	0	32	IV	Bad
Phyllite	47	S1 – 0.15	S1 – 1	S1 - -60	0			
		S2 – 0.70	S2 – 1	S2 - -6		38	IV	Bad
		S3 – 0.15	S3 – 0.85	S3 - -60				
Graphite Schist	47	S1 – 0.15	S1 – 1	S1 - -60	0			
		S2 – 0.85	S2 – 1	S2 – 0				
		S3 – 0.15	S3 – 0.85	S3 - -60		38	IV	Bad
Garnetiferous Schist	42	S1 – 0.15	S1 – 1	S1 - -60	0			
		S2 – 0.85	S2 – 1	S2 – 0				
		S3 – 0.15	S3 – 0.85	S3 - -60		33	IV	Bad
Calc-Schist	67	S1 – 0.15	S1 – 1	S1 - -60	-8			
		S2 – 1	S2 – 1	S2 – 0				
		S3 – 0.15	S3 – 1	S3 - -60		35	IV	Bad
		S4 – 0.40	S4 – 1	S4 - -60				
Quartzite	68	S1 – 0.15	S1 – 1	S1 - -60	-8			
		S2 – 0.85	S2 – 1	S2 - -6				
		S3 – 0.15	S3 – 0.85	S3 - -60				
		S4 – 0.15	S4 – 1	S4 - -6		51	III	Normal
Carbo-	65	S1 – 0.15	S1 – 1	S1 - -60	-8			

Rock type	No.					No.	Class	Rating
phyllite		S2 – 0.85; S3 – 0.15; S4 – 0.15	S2 – 1; S3 – 0.85; S4 – 1	S2 – -6; S3 – -60; S4 – 0		48	III	Normal
Flaggy quartzite	33	S1 – 0.15; S2 – 0.15; S3 – 0.15	S1 – 1; S2 – 1; S3 – 0.85	S1 – -60; S2 – 0; S3 – -60	-8	16	V	Very Bad
Calc-schist	55	S1 – 0.15; S2 – 1; S3 – 0.15; S4 – 0.15	S1 – 1; S2 – 1; S3 – 0.85; S4 – 1	S1 – -60; S2 – -60; S3 – -60; S4 – -50	8	3	V	Very Bad
Flaggy Quartzite	44	S1 – 0.70; S2 – 0.15; S3 – 0.15; S4 – 0.15	S1 – 1; S2 – 1; S3 – 0.85; S4 – 1	S1 – -6; S2 – -50; S3 – -60; S4 – 0	-8	28	IV	Bad
Calcschist	50	S1 – 0.15; S2 – 0.15; S3 – 0.70; S4 – 0.15	S1 – 1; S2 – 1; S3 – 0.85; S4 – 1	S1 – -6; S2 – -50; S3 – -60; S4 – 0	-8	6	V	Very Bad
Chlorite schist	35	S1 – 0.15; S2 – 0.70; S3 – 0.15; S4 – 0.15	S1 – 1; S2 – 1; S3 – 0.85; S4 – 1	S1 – -50; S2 – -6; S3 – -60; S4 – -6	0	27	IV	Bad
Quartzite	61	S1 – 0.15; S2 – 1; S3 – 0.40; S4 – 0.15	S1 – 1; S2 – 1; S3 – 0.85; S4 – 1	S1 – -50; S2 – -6; S3 – -60; S4 – -6	-8	45	III	Normal
Amphibolite	72	S1 – 0.15; S2 – 0.15; S3 – 0.15	S1 – 1; S2 – 1; S3 – 0.85	S1 – -60; S2 – -60; S3 – -60	-8	55	III	Normal
Quartzite	72	S1 – 0.15; S2 – 0.15; S3 – 0.40	S1 – 1; S2 – 1; S3 – 0.85	S1 – -50; S2 – -25; S3 – -60	-8	43	III	Normal
Chlorite Schist	40	S1 – 0.15; S2 – 0.15; S3 – 0.40	S1 – 1; S2 – 1; S3 – 0.85	S1 – -50; S2 – -25; S3 – -60	0	19	V	Very Bad
Amphibolite	82	S1 – 0.15; S2 – 0.70; S3 – 0.15; S4 – 0.15	S1 – 1; S2 – 0.85; S3 – 0.85; S4 – 1	S1 – -60; S2 – -60; S3 – -60; S4 – -60	0	46	III	Normal
Chlorite Schist	40	S1 – 0.15	S1 – 1	S1 – -60	0	31	IV	Bad
Quartzite	67	S1 – 0.15; S3 – 0.15; S4 – 0.15	S1 – 1; S3 – 0.40; S4 – 1	S1 – 0; S2 – -60; S4 – 0	-8	55	III	Normal
Amphibolite	67	S1 – 0.15; S3 – 0.15; S4 – 0.15	S1 – 1; S3 – 0.70; S4 – 1	S1 – 0; S3 – -60; S4 – 0	-8	52	III	Normal
Quartzite	64	S1 – 0.15; S3 – 0.15; S4 – 0.15	S1 – 1; S3 – 0.40; S4 – 1	S1 – 0; S3 – -60; S4 – 0	-8	52	III	Normal
Amphibolite	65	S1 – 0.15; S2 – 0.15; S3 – 0.15; S4 – 0.15; S5 – 0.15	S1 – 1; S2 – 1; S3 – 0.40; S4 – 1; S5 – 0.85	S1 – -6; S2 – -60; S3 – -60; S4 – -50; S5 – -60	-8	48	III	Normal
Quartzite	68	S1 – 0.40	S1 – 1	S1 – -6	-8			

Table 4.10 – contd....

109

		S2 – 0.15 S3 – 0.15 S4 – 0.15 S5 – 0.15	S2 – 1 S3 – 0.40 S4 – 1 S5 – 0.85	S2 - -6 S3 - -60 S4 - -6 S5 - -60		52	III	Normal
HIGHER HIMALAYAN CRYSTALLINES								
Biotite Gneiss	54	S1 – 0.15 S2 – 0.15 S3 – 0.15 S4 – 0.15	S1 – 0.85 S2 – 1 S3 – 1 S4 – 1	S1 - -60 S2 - -50 S3 – 0 S4 – 0	-8	38	IV	Bad
Amphibolite	50	S1 – 0.15 S3 – 0.15 S4 – 0.15	S1 – 1 S3 – 0.85 S4 – 1	S1 - -60 S3 - -60 S4 - -50	-8	33	IV	Bad
Migmatised Gneiss	87	S1 – 0.15 S2 – 0.15 S3 – 0.15	S1 – 1 S2 – 1 S3 – 1	S1 - -25 S2 - -6 S3 - -60	8	70	II	Good
Amphibolite	63	S1 – 0.15 S3 – 0.15 S4 – 0.40	S1 – 1 S3 – 1 S4 – 1	S1 - -60 S3 - -60 S4 - -50	-8	35	IV	Bad
GM Schist	24	S1 – 0.15	S1 – 1	S1 - -50	0	16	V	Very Bad
Amphibolite	63	S1 – 0.15 S3 – 0.15 S4 – 0.40	S1 – 1 S3 – 1 S4 – 1	S1 - -60 S3 - -60 S4 - -50	-8	35	IV	Bad
Biotite Gneiss	45	S1 – 0.15 S2 – 0.15 S3 – 1 S4 – 0.15	S1 – 0.85 S2 – 1 S3 – 1 S4 – 1	S1 - -50 S2 – 0 S3 – 0 S4 – 0	-8	30	IV	Bad
Amphibolite	63	S1 – 0.15 S3 – 0.15 S4 – 0.40	S1 – 1 S3 – 1 S4 – 1	S1 - -60 S3 - -60 S4 - -50	-8	35	IV	Bad
Migmatised Gneiss	87	S1 – 0.15 S2 – 0.15 S3 – 0.15	S1 – 1 S2 – 1 S3 – 1	S1 - -25 S2 - -6 S3 - -60	8	70	II	Good
Biotite Gneiss	45	S1 – 0.15 S2 – 0.15 S3 – 1 S4 – 0.15	S1 – 0.85 S2 – 1 S3 – 1 S4 – 1	S1 - -50 S2 – 0 S3 – 0 S4 – 0	-8	30	IV	Bad
GM Schist	24	S1 – 0.15	S1 – 1	S1 - -50	0	16	V	Very bad
Amphibolite	63	S1 – 0.15 S3 – 0.15 S4 – 0.40	S1 – 1 S3 – 1 S4 – 1	S1 - -60 S3 - -60 S4 - -50	-8	35	IV	Bad
Biotite Gneiss	45	S1 – 0.15 S2 – 0.15 S3 – 1 S4 – 0.15	S1 – 0.85 S2 – 1 S3 – 1 S4 – 1	S1 - -50 S2 – 0 S3 – 0 S4 – 0	-8	30	IV	Bad
GM Schist	24	S1 – 0.15	S1 – 1	S1 - -50	0	16	V	Very bad

Note: *Stretch 1-15 are Scanline Survey locations at intervals of every 500m starting from Tawaghat towards Jipti.*
GM Schist – Garnet Mica Schist

However, because of physical limitations and economic constraints, all parameters cannot be measured with equal ease and success. The focus of this write-up is primarily highlighting field instrumentation and measurement techniques adopted to study Mangti Landslide through in-situ installation of Open Stand-pipe Type Piezometer for measurement of pore-water pressure and the movement monitoring devices (rods) for vectoral measurement of shallow sub-surface ground-displacement.

Such field instrumentation is most oftenly used on landslides that have already exhibited some movement. In such cases the overall dynamic characteristics of the landslide are frequently and readily observed and recorded. However, small movements of a soil or rock mass before or even during incipient slope failure are usually not visually evident. Thus, the value of the information that can be obtained at the ground surface is limited. Instrumentation can provide valuable information on incipient as well as fully developed landslides. In this respect, use of instrumentation is not intended to replace field observations and other investigative procedures. Instead, it augments other data by providing supplementary information and by warning of impending major movements (Mikkelsen, 1996).

The Mangti Landslide constitutes as the most young and active landslide. Field instrumentation installed at Mangti Landslide was setup with a view to gather information on the following parameters –

> Determination of the depth and shape of the sliding mass in a developed landslide with a view to define appropriate strength parameters at failure and design remedial measures,

> To monitor and quantify absolute lateral and vertical movements within a sliding mass,

> To estimate the rate of mass movement,

> Monitoring of the slope activity of marginally stable natural / cut slopes and identification of effects of precipitation,

> Monitoring of groundwater activity / pore water pressure normally associated with slope mass movement so as to perform effective stress analysis,

There exists large variety of instruments involving sophisticated real-time monitoring of landslide coupled with warning alarm system to simple instrumentation providing in-situ parameters on stress behaviour as well as quantification of slope mass movement.

Owing to the complexity of the landslide material comprising massive boulders inter-mixed with sandy matrix, drilling through the soil mass till the bedrock was not possible. On prolonged observation of the kind of movement seen at Mangti Landslide it could be discerned that failure of slope mass is initiated at the point when entire landslide mass gets saturated. Since the landslide mass constitutes of boulder-sand mixture, groundwater percolates and drains very fast as it has high permeability and time of pore-water pressure built-up is extremely short. Looking to the above fact the investigation was restricted for the in-situ field instrumentation activity to a shallow subsurface regime only and using cost-effective, more conventional monitoring techniques.

PIEZOMETER INSTALLATION FOR PORE-WATER PRESSURE MEASUREMENTS

In slope mass failure, groundwater activity through pore water pressure act as the foremost important triggering factor. Measurement of internal pore water pressure at various critical points in the landslide body as well as adjacent shoulder regions has been considered as vital field observations that are required to study the behaviour of slope mass, which infact is a function of materials shearing strength (Terzaghi, 1950). Shearing strength of soil is dependent primarily on the normal or confining stress. Under this stress, the soil grains are forced into more intimate contact and the volume of the soil mass is decreased somewhat. Since the volume of the soil grains cannot be changed appreciably, this volume change must take place primarily in the voids or pore of the soil. If these pores are completely filled with water, their volume cannot be changed unless some of the water is drained from the soil mass. If drainage is prevented a stress will be developed in the pore water

112

opposing the externally applied stress. The developed stress is called *pore-water pressure*. Since the pore-water pressure is opposed to the normal or confining stress, the shearing resistance will be reduced whenever positive pore-water pressure is present. This relation is shown in Equation 3 –

$$S = C + (\sigma - U) \tan \emptyset \qquad (3)$$

Where, S = *Shearing Strength*, σ = *Normal Stress on Sliding Surface*, C = *Cohesion*, U=*Pore-water Pressure* and tan $\emptyset$ = *Coefficient of Internal Friction*.

These pore pressure values measured with the help of Piezometers define the areas where pore-fluid pressure will affect the stability of the slope adversely during and after monsoons.

Decrease in shear strength with time may be ascribed to change in fabric character, removal of overburden and/or subsequent swelling. These factors are greatly influenced by the available moisture content and the stress exerted by the water molecules in the interstitial spaces. The changing behaviour of pore water pressure under any event or process viz. Rain, frost or dry spell, causes adverse effects on equilibrium conditions of slope leading to decrease in frictional resistance and cohesion (Terzaghi, 1950). Therefore, realizing the importance of pore water pressure as triggering factor, the author has made an attempt to study this vital aspect.

As it has already been stated that the activity of Mangti Landslide is predominantly witnessed during monsoon season and water-table drastically lowers down after monsoon, therefore, it has been considered appropriate to go for installation of shallow Open Stand Pipe Casagrande Piezometers (Wilson and Mikkelsen, 1978). **Piezometer** *is an instrument for measuring pressure head of flowing water within regolith and or rock masses. It usually consists a small sized pipe tapped into the sides of a closed or open conduit and flush with the inside – connected with a pressure gauge, water column for indicating pressure head.*

The Open Stand Pipe Casagrande Piezometer for determining soil pore water pressure is used because of its simplicity, cost effectiveness and reliability in comparison with transducer type instruments. Such factors are especially relevant

when instrumentation is used on remote and inaccessible sites like Mangti Landslide. Although the Casagrande type systems relate to poor response times (Time-Lag) particularly in soils of low permeability (Hvorslev, 1951), the response can be improved by taking the design of installation into consideration in terms of the Piezometers' collection area and standpipe size.

Time-lag measures the sensitivity of the Piezometers i.e., the length of time required for the Piezometers to equalize after a change of pressure. This time lag is directly proportional to the cross sectional area of the stand pipe and varies inversely with the permeability of the surrounding soils. Therefore, sensitivity of the Piezometers can be increased by lengthening the porous space and up to somewhat by increasing its diameter, less the time-lag, more sensitive will be the instrument. Also, Open Stand Pipe Piezometers are best suited for relatively permeable soil ($K=10^{-4}$ cm/sec), if time lag is to be kept within reasonable time limits say 2 – 4 hours (Hvorslev, 1951).

The layout plan giving details on Piezometer locations, adopted Piezometers design etc. is furnished in Figure 4.9. The entire activity of Piezometer installation has been carried out with the active support of BRO – GREF staff and by adhering the procedures recommended in Indian Standard Code of Practice [IS: 7356 (Part-I) – 1974].

Step by step account on adopted methodology in Piezometer installation is given as under-

Step – 1   Excavation of pits of at least 2.50m depth and 30" diameter at its base. Sampling of sediments at every 30cm depth or change of strata, which ever is earlier.

Step – 2   Cleaning of pit and lowering of 100mm Ø perforated and wire mesh wrapped PVC pipe, followed by sand filling up to 60cm from pit base and pulling the pipe upward 30cm to create filter base below the perforated zone.

Step – 3   Filling of additional sand up to 30cm above the perforation zone and sealing by Bentonite cake, i.e., 30cm above sand filter.

114

Step – 4 Filling of earth up to the ground surface and making concrete platform

Step – 5 Time lag observations (Hvorslev, 1951) using electrical probe for evaluation of Piezometer performance and determining the in-situ permeability of the slope mass.

Pictorial depiction of step by step Piezometer installation activity is shown in (Plate IV.4). Time lag observations have been carried out to evaluate Piezometers' performance as per theoretical and experimental methods presented by Hvorslev (1951). During the advancement of a borehole or immediately after installation of a pressure measuring device, the hydrostatic pressure within the hole or device is seldom equal to the original pore-water pressure. A flow of water to or from the bore hole or pressure measuring device then takes place until pressure difference are eliminated and the time required for practical equalization of the pressures i.e. the *time-lag*. Permeability of the soil significantly influences the hydrostatic pressure equalization between the pressure monitoring device and the surrounding environment. The soil structure is often disturbed and the stress conditions are changed by advancing a bore hole or driving a well/pit for installation of pressure monitoring devices. This causes a transient change in the void ratio and water content of the soil and indirectly modifies the permeability of soil to some extent in the surrounding region of pressure device. Hence, utmost care was taken during the installation of Piezometers and the pits were refilled with the same slope material so that the errors caused in hydrostatic time-lag and stress adjustment time-lag would be minimal.

With the help of time-lag observations in-situ coefficient of permeability 'k' can be evaluated theoretically in field. The theoretical derivation below shows mathematical equation used in calculating infield permeability (Hvorslev, 1951) –

The flow rate (q) into the Piezometer can be expressed as in Equation 4,

$$q = F.k.H \qquad (4)$$

Where,

F = the shape factor of the Piezometer tip,

k = coefficient of permeability;   H = head of ground water

The total volume of water required for equalization of the pressure difference, H, is given by the Equation 5,

$$V = A.H \qquad (5)$$

Where, 'A' is cross-sectional area of the standpipe. Thus the basic time-lag 'T' (Equation 6) can be defined as the time required for equalization of this pressure difference when the original rate of flow, q = FkH, is maintained; that is

$$T = V/q = A.H / F.k.H = A / F.k \qquad (6)$$

and the coefficient of permeability then can be written as in Equation 7,

$$k = A / F.T \qquad (7)$$

It is probable that the time-lag during normal operating conditions corresponds to an equalization diagram, which for practical purposes may be represented by a straight line through the origin and then running parallel to the X-axis of the diagram obtained in time-lag tests as shown in Figure 4.10.

The time lag observation results (Figure 4.10) has provided highly satisfactory results showing Piezometers' response within the time range of 25 – 60 minutes for stress adjustment. Based on Hvorslev's (1951) plots, sub-surface in-situ permeability fall in the range of 10^{-2} to 10^{-4} cm/sec. This obtained permeability range is in conformation with the granulometric characteristics of the sediment samples falling in GP – SP – SM groups and indicative of sandy nature (Figure 4.11).

B. Making of 3mm Φ Perforation in PVC Pipe

D. Emplacing the perforated pipe wrapped with wire mesh on a base of 30cm sand filter column.

Plate IV.4 – contd.....

A. Excavation of pit at critical locations in active landslide region
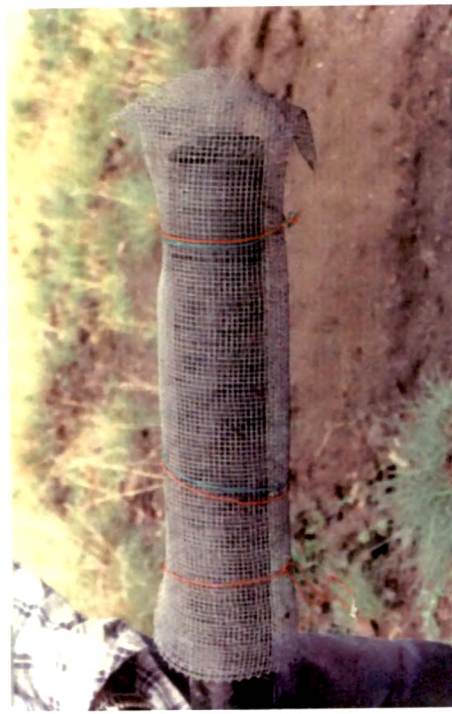
C. Wrapping up the perforated area with wire mesh to avoid entering of sand particles into the Piezometer device.

117

F. Sealing the total 90cm sand filter column with Bentonite Plug to restrict vertical percolation of water into the Piezometer device

H. Performing Time-Lag observation for evaluation of Piezometer performance and determining the in-situ permeability of the slope mass

E. Covering with sand from the base of perforation to make a 60cm sand filter column around the perforated pipe section

G. Refilling the pit and sealing it with cement then carrying out saturation around the device by filling in water

Plate IV.4 - Chronological Depiction of Open Stand Pipe Type Piezometer Installation at Mangti Landslide
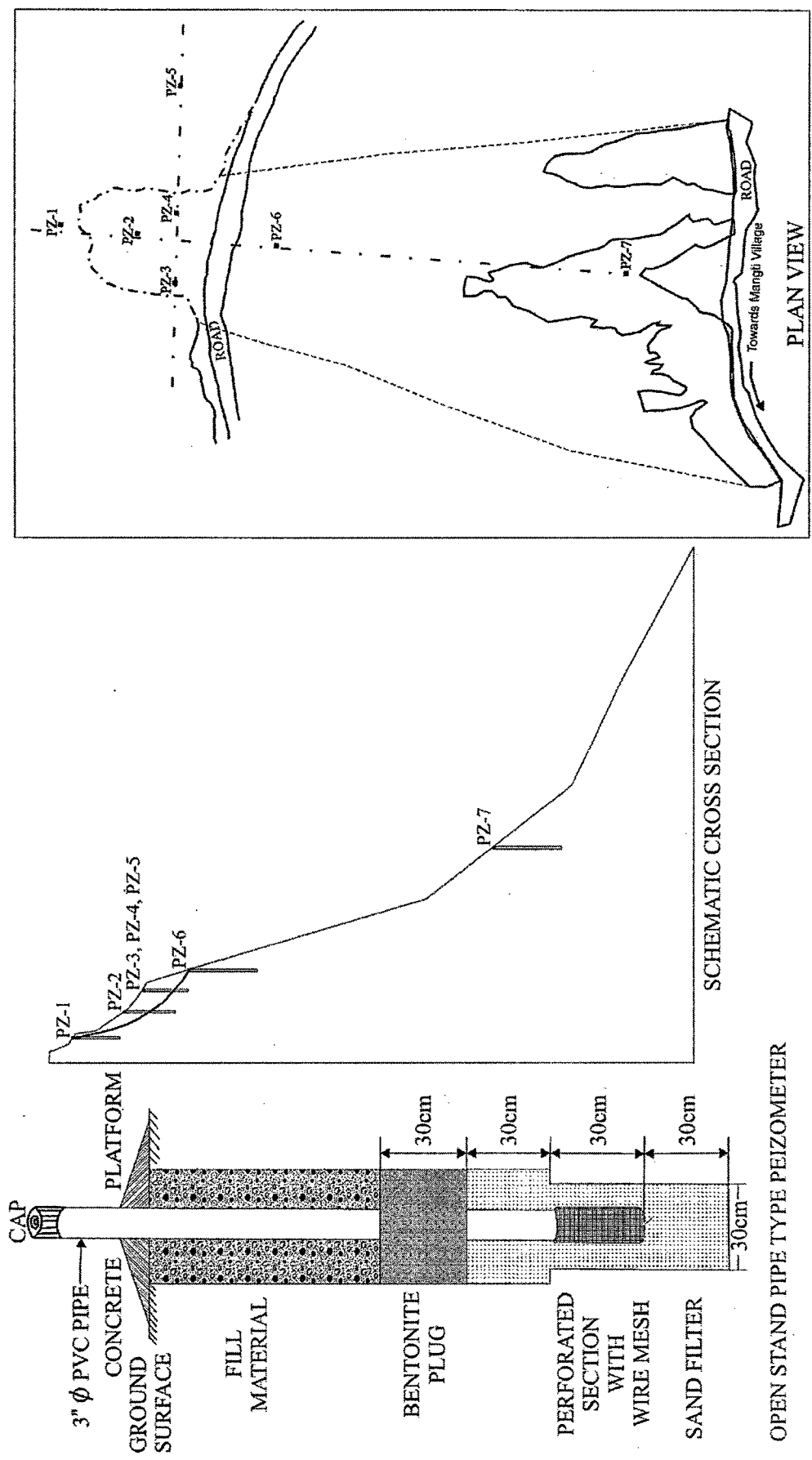
Figure 4.9 - Location Plan of Installed Open Stand Pipe Type Piezometers – Mangti Landslide
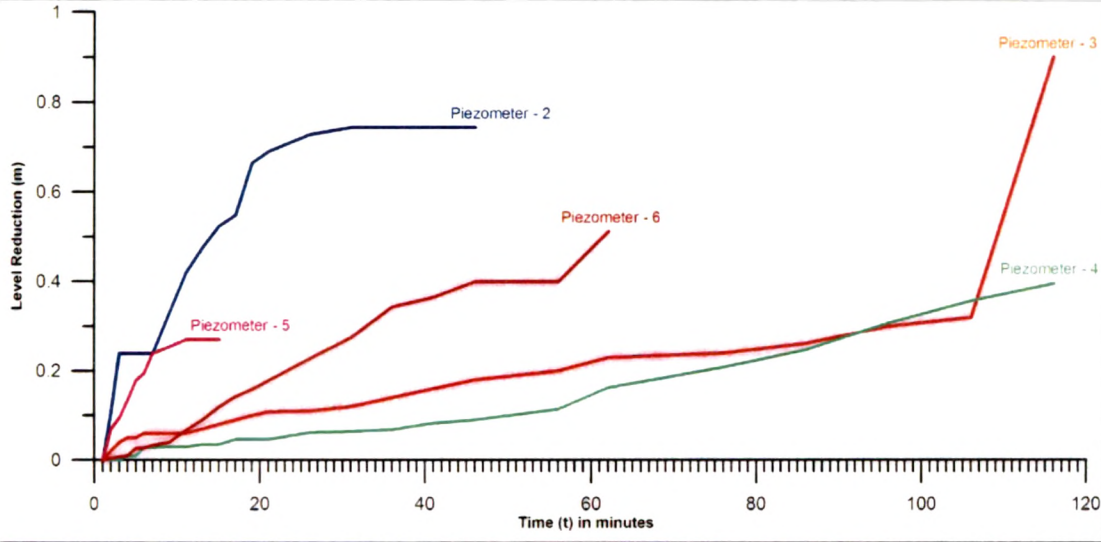
Figure 4.10 - Time-lag Observation Plot of the Piezometers, Mangti Landslide.
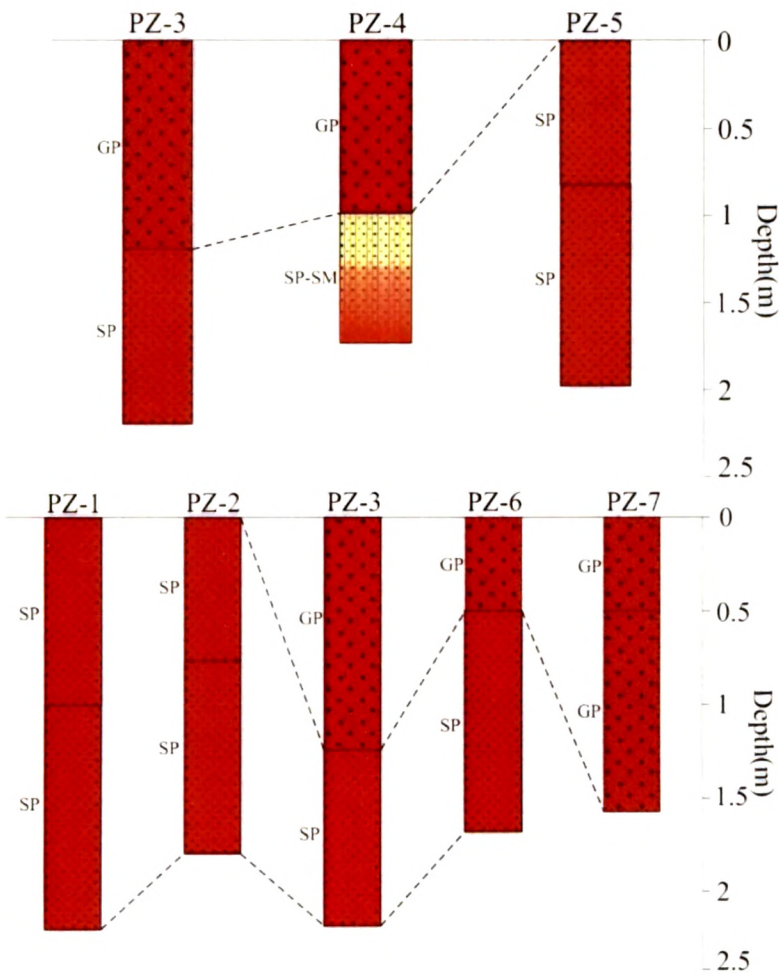
Figure 4.11 - Subsurface Profiles Along Installed Piezometers – Mangti Landslide.

120

INSTALLATION OF SHALLOW SUB-SURFACE MOVEMENT MONITORING DEVICES (RODS) FOR GROUND-DISPLACEMENT MEASUREMENTS

Quantitative assessment (vectoral measurement) of slope mass movement within the landslide zone and adjacent shoulder regions has been made using traditional method of inserting metal rods in slope mass (Keaton and Degraff, 1996). Entire activity has been performed in following steps:

Step-1: Selection of location spots for fixing the movement monitoring rods encompassing the regions like crown, main body of landslide that includes zone of ablation and zone of accumulation, adjacent shoulder regions. In all 16 numbers of locations for the ongoing 3rd phase of landslide has been taken up (Figure 4.12).

Step–2: Excavation of pits of 50cm depth and fixing of 2m long (1.5m free length) half inch diameter G.I. pipe using cement-sand-concrete mixture.

Step–3: Painting and numbering of the movement monitoring rods.

Step–4: Recording the initial position of these rods from fixed position platforms using Total Station and geographical positions using Differential Global Positioning System for Latitude, Longitude and Elevation.

Step–5: Monitoring of device positions first on monthly basis (non-monsoon period) and then on weekly basis (Monsoon Period) using electronic Total Station.

Field photographs depicting step by step procedure of this activity is shown in Plate IV.5A-D. Similarly changes perceived by landslide morphology particularly within the zone of ablation and mass accumulation have been monitored using electronic Total Station from fixed locations. The details on observed surface movements for the period of 02 years (2003-2005) of the various movement devices through vector diagram (Figure 4.12) and the observed change in landslide morphology for the same period is given in Figure 4.13.

LANDSLIDE KINEMATICS

The kinematics of a landslide – how movement is distributed through the displaced mass is one of the principal criteria for classifying landslides. However, of equally great importance is its use as a major criterion for defining the appropriate response to a landslide (Cruden and Varnes, 1996). For instance, occasional falls from a rock

cut adjacent to a highway may be contained by a rock fence or similar barrier; in contrast, toppling from the face of the excavation may indicate adversely oriented discontinuities in the rock mass that require anchoring or bolting for stabilization.

The vector diagram (Figure 4.14) clearly depicts that the overall rate of mass movement is more than 05 times (22.91 cm) on the right side half and shoulder region of the landslide with significant subsidence (-8.96 cm) as well as rise in the way of ground heaving (+4.68 cm) than what is observed in its counter left side half (Plate IV.6L). This differential behaviour in vector patterns may be attributed to difference in the material characteristics viz. composition, lateral continuity, hydraulic properties, etc.

Through monitoring of changes in morphology of Mangti Landslide for a prolonged period of two years has bestowed some remarkable details on its evolution and development. Mangti Landslide can be classified as *Very Slow* moving *Debris Slide* which at times of intense rainfall event exhibits *Very Rapid* movement (Varnes, 1978). It moves along a surface of rupture that is curved and concave with little internal deformation. The head of the displaced material moves almost vertically downward whereas the upper surface of the displaced material tilts backward towards the scarp. The scarp below the crown is almost vertical and unsupported. Further movements have caused retrogression of the slide into the crown. The lateral margin of the surface of rupture is sufficiently high and steep to cause the flanks to move down and into the depletion zone of the slide. Kinematic study of Mangti Landslide through surface movement suggests that the mass movement activity is mainly confined to rainy season when the groundwater movement charges the slope mass, through in-building of pore water pressure and on attaining saturation. This phenomenon has been physically witnessed after an event of rainfall, leading to rapid flow of saturated mass that had necessitated engaging labour force & Bull dozer to clear the road (Plate IV.6F).A sequence of photographs monitoring the third phase of movement in Mangti Landslide between June 2003 to September 2005 depicting changes in the crown, scarp and body morphology of the landslide is shown in Plate IV.6.

A. Fixing of movement monitoring rod with concrete mix

B. View of horizontal row of installed movement monitoring rod in active landslide region

C. View of giving finishing touches to installed movement monitoring rods for distant visibility

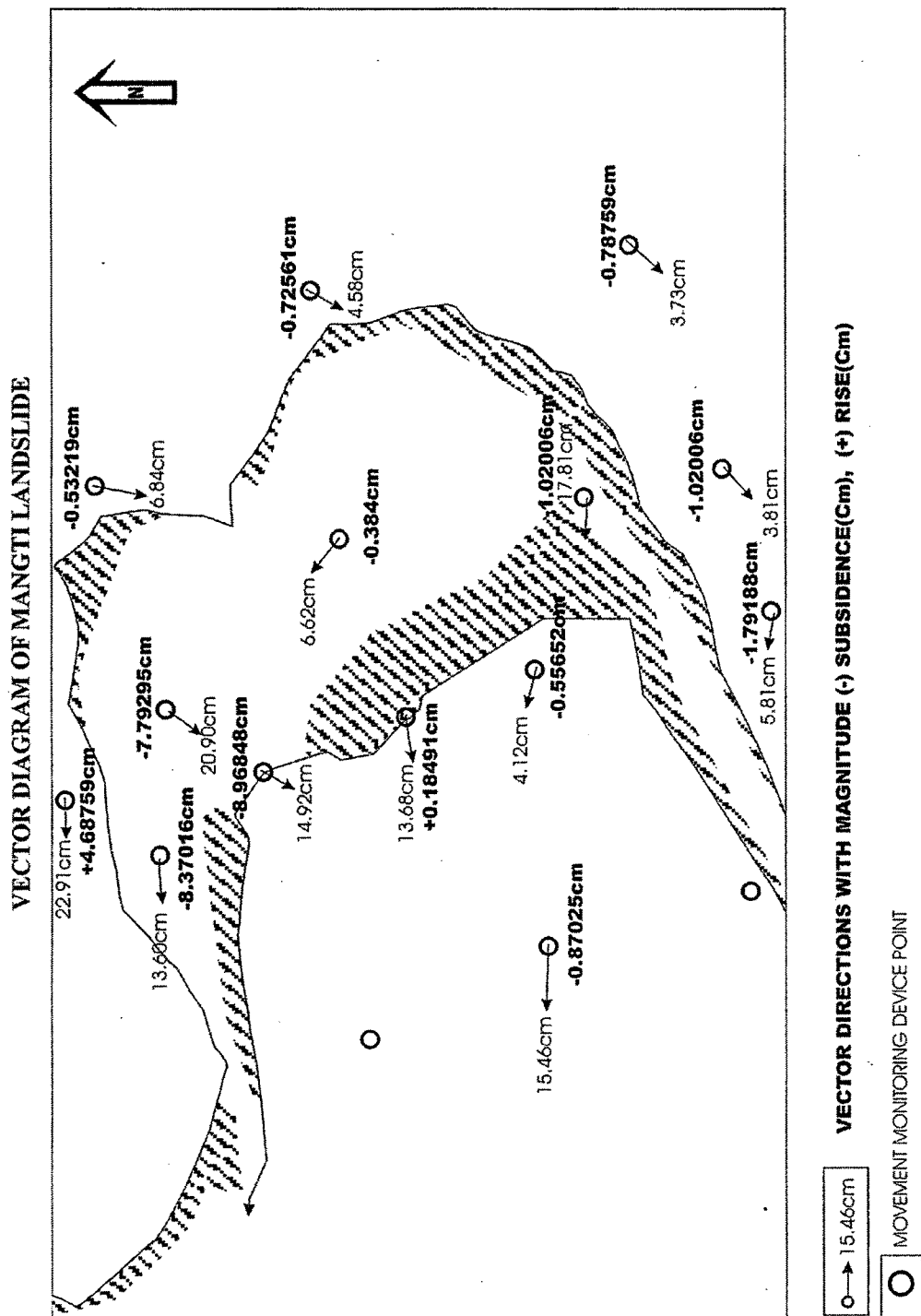**Plate IV.5-Sequential Photographs of Movement Monitoring Rods Installation Procedure**

VECTOR DIAGRAM OF MANGTI LANDSLIDE

Figure 4.14 - Vector Diagram on Observed Mass Movement, Mangti Landslide

VECTOR DIRECTIONS WITH MAGNITUDE (-) SUBSIDENCE(Cm), (+) RISE(Cm)

o——→15.46cm

O MOVEMENT MONITORING DEVICE POINT

NORTHING (m)

EASTING (m)

LEGEND

Landslide periphery in
Aug-Sep 2005

Landslide periphery in
Nov-Dec 2003

Towards Jiptii Village

Towards Mangti Village

N

6400 6350 6300 6250 6200 6150 6100 6050 6000

4050 4000 3950 3900
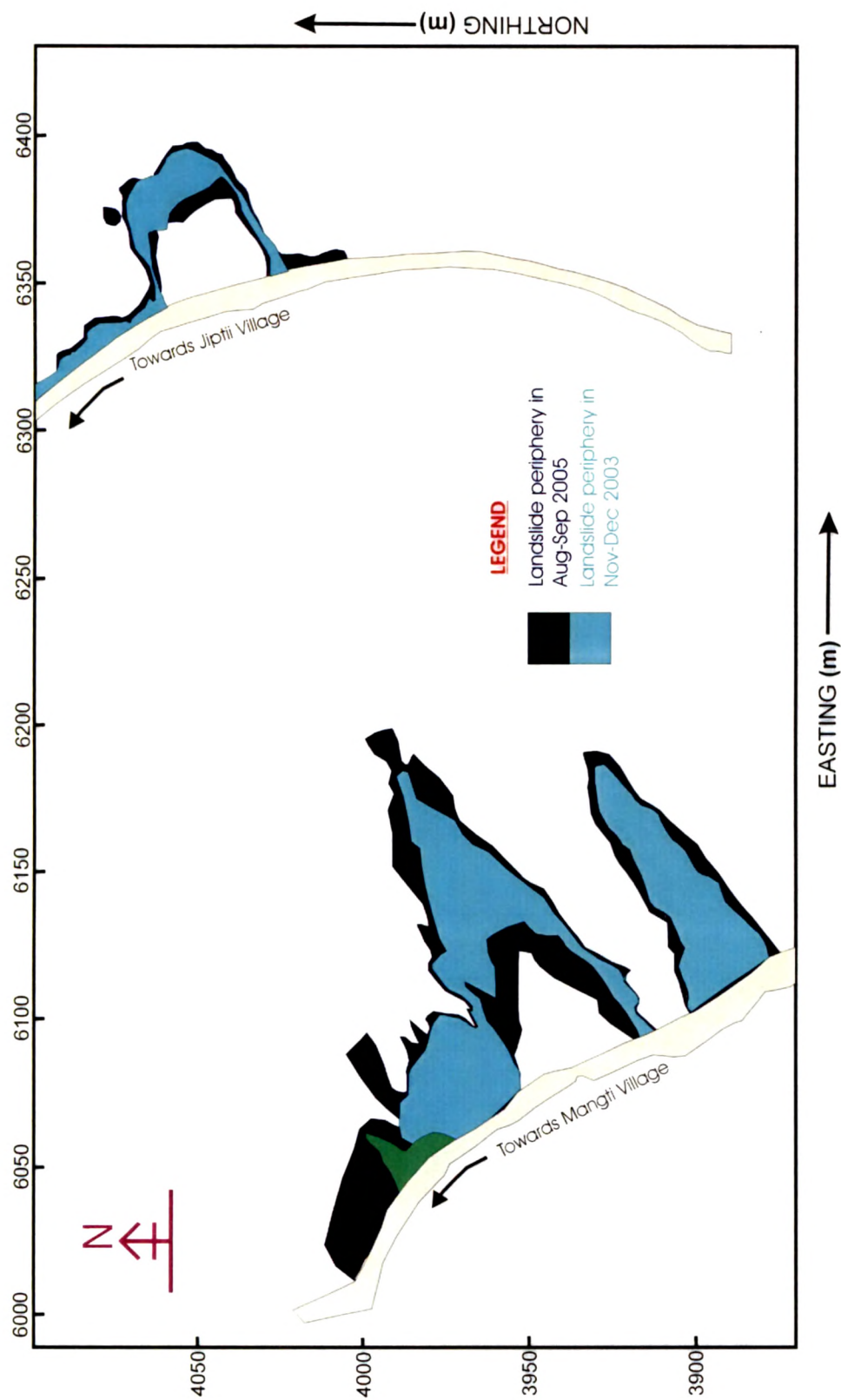
Figure 4.15 - Observed Annual Peripheral Changes in Mangti Landslide

B. View of right side of the crown and right flank on the upper 3rd stage of slope failure in Mangti Landslide (jan. 2003)
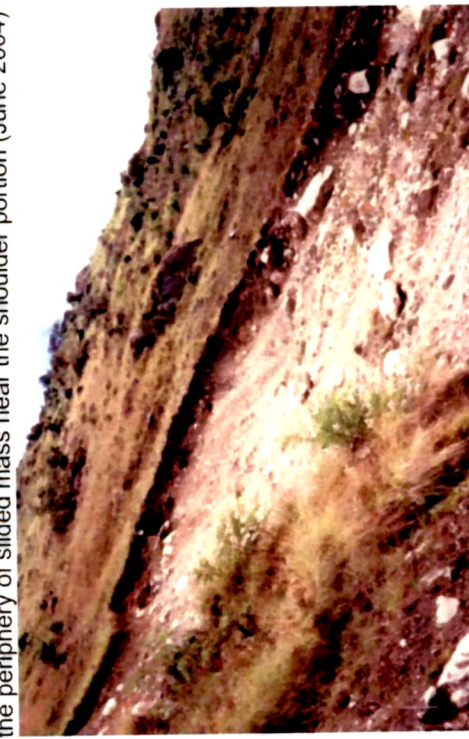

D. View of the crown portion of upper 3rd stage of slope failure in Mangti Landslide (Nov. 2003)

Plate IV.6 – contd....

A. Frontal view of lower portion of Mangti landslide (Jan. 2003). Blue line demarcates the boundary of slided mass.
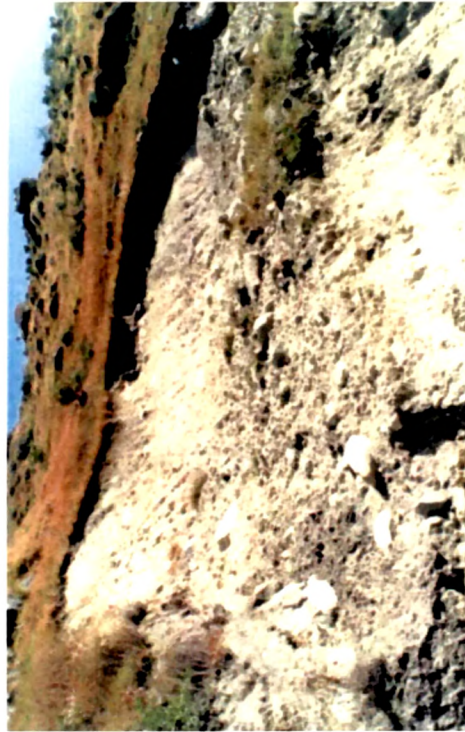
C. View of left side of the crown and left flank on the upper 3rd stage of slope failure in Mangti Landslide (Nov. 2003)

126

F. View of labourers clearing the slide debris from the road (July 2004)

H. View of the Debris flow witnessed in Mangti landslide after complete saturation of the slope mass (Sep. 2004)

Plate IV.6 – contd.....

E. Side view of Mangti Landslide from GREF Camp. Blue line shows the periphery of slided mass near the shoulder portion (June 2004)

G. View of left side of the crown and left flank on the upper 3rd stage of slope failure in Mangti Landslide (Sep. 2004). Remarkable change in the slope angle of main scarp is observed.

J. Side view of Mangti Landslide from GREF Camp. Blue line shows the periphery of slided mass near the shoulder portion (June 2005)

L. Heaving of slope mass in accumulation zone along the left shoulder portion of the upper level of Mangti Landslide is observed (Sep. 2005)

A noteworthy observation of advancing landslide periphery appears to be evident from repetitive surveillance made at the Landslide.

Plate 4.6 - Sequence of Field Photographs Monitoring the Third Phase of Movement in Mangti Landslide between January 2003 to September 2005

I. Frontal view of lower portion of Mangti landslide (June. 2005). Blue line demarcates the boundary of slided mass.

K. Distant view of upper level of Mangti Landslide. Lateral advancement of the slide zone can be observed (June 2005)

128